NAVAL
POSTGRADUATE
SCHOOL

MONTEREY, CALIFORNIA

THESIS

DISTRIBUTED SUBARRAY ANTENNAS FOR MULTIFUNCTION PHASED-ARRAY RADAR

by

Chih-heng Lin

September 2003

Thesis Advisor:	David Jenn
Second Reader:	Richard Adler

Approved for public release, distribution is unlimited

THIS PAGE INTENTIONALLY LEFT BLANK

REPORT DOCUMENTATION PAGE			Form Approved OMB No. 0704-0188
Public reporting burden for this collection of information is estimated to average 1 hour per response, including the time for reviewing instruction, searching existing data sources, gathering and maintaining the data needed, and completing and reviewing the collection of information. Send comments regarding this burden estimate or any other aspect of this collection of information, including suggestions for reducing this burden, to Washington headquarters Services, Directorate for Information Operations and Reports, 1215 Jefferson Davis Highway, Suite 1204, Arlington, VA 22202-4302, and to the Office of Management and Budget, Paperwork Reduction Project (0704-0188) Washington DC 20503.			
1. AGENCY USE ONLY *(Leave blank)*	**2. REPORT DATE** September 2003	**3. REPORT TYPE AND DATES COVERED** Master's Thesis	
4. TITLE AND SUBTITLE: Distributed Subarray Antennas for Multifunction Phased-Array Radar			**5. FUNDING NUMBERS**
6. AUTHOR (S) Chih-heng Lin			
7. PERFORMING ORGANIZATION NAME (S) AND ADDRESS (ES) Naval Postgraduate School Monterey, CA 93943-5000			**8. PERFORMING ORGANIZATION REPORT NUMBER**
9. SPONSORING /MONITORING AGENCY NAME (S) AND ADDRESS (ES) N/A			**10. SPONSORING/MONITORING AGENCY REPORT NUMBER**
11. SUPPLEMENTARY NOTES The views expressed in this thesis are those of the author and do not reflect the official policy or position of the Department of Defense or the U.S. Government.			
12a. DISTRIBUTION / AVAILABILITY STATEMENT Approved for public release, distribution is unlimited			**12b. DISTRIBUTION CODE**

13. ABSTRACT ***(maximum 200 words)***

As the target radar cross section (RCS) continuously decreases, the need for high-resolution high-gain radar increases. One approach to high resolution is to use distributed subarray antennas (DSAs), because of limited surface available on many radar platforms.

The concept of distributed subarray antennas is examined for both Multifunction Array Radar (MFAR) and Very High Frequency (VHF) applications. By combining distributed subarrays located on the available areas of a constrained platform, the MFAR and VHF DSA can achieve increased resolution and potential reductions in cost and complexity compared to a conventional array. The two-way pattern design of DSA effectively suppresses the undesired grating lobes by using separate transmit and receive antennas. By the pattern multiplication principle, the grating lobes in the subarray receive pattern have been suppressed by proper null placement of subarray in the receive and transmit antenna patterns.

14. SUBJECT TERMS Phased Array, Subarray, Multifunction Array Radar (MFAR), Two-way Gain.			**15. NUMBER OF PAGES** 89
			16. PRICE CODE
17. SECURITY CLASSIFICATION OF REPORT Unclassified	**18. SECURITY CLASSIFICATION OF THIS PAGE** Unclassified	**19. SECURITY CLASSIFICATION OF ABSTRACT** Unclassified	**20. LIMITATION OF ABSTRACT** UL

NSN 7540-01-280-5500 Standard Form 298 (Rev. 2-89)
Prescribed by ANSI Std. 239-18

THIS PAGE INTENTIONALLY LEFT BLANK

Approved for public release, distribution is unlimited

DISTRIBUTED SUBARRAY ANTENNAS FOR MULTIFUNCTION PHASED-ARRAY RADAR

Chih-heng Lin
Lieutenant Commander, Taiwan Navy
B.S., Chinese Naval Academy, 1990

Submitted in partial fulfillment of the
requirements for the degree of

MASTER OF SCIENCE IN SYSTEM ENGINEERING

from the

NAVAL POSTGRADUATE SCHOOL
September 2003

Author: Chih-heng Lin

Approved by: David C. Jenn
Thesis Advisor

Richard W. Adler
Second Reader

Dan Boger
Chairman, Department of Information Sciences

THIS PAGE INTENTIONALLY LEFT BLANK

ABSTRACT

As the target radar cross section (RCS) continuously decreases, the need for high-resolution high-gain radar increases. One approach to high resolution is to use distributed subarray antennas (DSAs), because of limited surface available on many radar platforms.

The concept of distributed subarray antennas is examined for both Multifunction Array Radar (MFAR) and Very High Frequency (VHF) applications. By combining distributed subarrays located on the available areas of a constrained platform, the MFAR and VHF DSA can achieve increased resolution and potential reductions in cost and complexity compared to a conventional array. The two-way pattern design of DSA effectively suppresses the undesired grating lobes by using separate transmit and receive antennas. By the pattern multiplication principle, the grating lobes in the receive pattern have been suppressed by proper null placement of subarray in the receive and transmit patterns.

THIS PAGE INTENTIONALLY LEFT BLANK

TABLE OF CONTENTS

LIST OF FIGURES

LIST OF TABLES

THIS PAGE INTENTIONALLY LEFT BLANK

ACKNOWLEDGMENTS

I would like to express my most sincere gratitude to Professor David Jenn of the Naval Postgraduate School, Monterey, California for his guidance and invaluable contributions to the completion of this work. Without his instruction I could not finish this work. I would also like to thank Professor Richard Adler for agreeing to be the second reader to the thesis. Both of them have prepared me in electromagnetics and antenna theory while I was in Naval Postgraduate School and the knowledge acquired has allowed me to proceed with the thesis work.

THIS PAGE INTENTIONALLY LEFT BLANK

I. INTRODUCTION

A. REQUIREMENTS AND OBJECTIVES

The platform design of future surface combatants has changed dramatically with the advent of stealth technology to reduce platform signatures. The change in design philosophy is evident in the proposed new DD-21, as illustrated in Figure 1. The traditional small-integrated superstructure of vessels allowed few areas for sensors and weapon systems. On the other hand, the threat from the air or surface is ever increasing such that the performance of shipboard radar needs to provide long-range detection and accurate tracking. This implies high gain and physically large radar antennas.

Since it is difficult to find a sufficient area for a large array onboard a ship, it might be possible to use several smaller noncontiguous (separated) areas (subarrays) and then process the received signal coherently. The subarrays may be far apart in terms of wavelength and therefore grating lobes occur. Grating lobes are undesirable because they reduce the antenna efficiency, cause ambiguities in angle measurements and make the radar more susceptible to jammers. They also complicate clutter processing.

The main objective of this thesis is to investigate a conceptual design of integrated antenna apertures, which are composed of several distributed noncontiguous subarrays. Together the entire set forms a Multi-function Array Radar (MFAR) antenna that provides multi-tasking with high-resolution high-speed data collection simultaneously. This thesis will show the trade-off in performance and cost for several possible antenna concepts.

One possible approach to achieving a large distributed array that is free of grating lobes is to design separate receive and transmit antennas. For example, the transmit antenna might consist of distributed subarrays. Then a separate receive antenna would be used whose pattern has nulls in the direction of the transmit array's grating lobes. Therefore the round trip or "two way" gain pattern would be free of grating lobes.

Figure 1. The Artist's concept of the DD-21 [Ref. 1]

This approach is difficult enough for narrow band radar. However, new antenna designs must provide wideband performance. Furthermore, due to the limited space, it is desired that the antenna serve as many systems as possible: several radars, communications systems, and electronic warfare systems. Ideally, the antenna should have the following characteristics:

1. Capability to execute different tasks in rapid sequence

All sensors and electronic devices need to be integrated into the small topside of the platform, and the integrated MFAR should have surveillance, tracking, identification, fire control, missile guidance and communication capabilities. The bandwidth of the MFAR, therefore, must be wide enough to provide good range resolution and to satisfy the requirements of different systems. The aperture size of the MFAR must be electrically large enough to give fine angle resolution and high directivity. The side lobes of the

antenna pattern, of course, have to be low enough to help distinguish the target from the natural or man-made clutter.

2. Capability for adaptive digital beamforming (ADBF)

Digital beamforming (which requires a modulator or demodulator at each element) is preferred. However, the large number of array elements required for high resolution reduces the possibilities of element-level digital beamforming considerably. The subarray-level ADBF could provide multiple beams and electronic scanning to carry out the multi-tasks simultaneously using a minimum number of control elements. The MFAR tracks targets accurately with low sidelobe sum and difference beams, which are required for monopulse tracking. There are also some other important features that could be provided by ADBF:

(1) Self-calibration and error correction
(2) Adaptive nulling of unwanted interference or jamming signals
(3) Spatial control of the radiated energy for Low Probability of Intercept (LPI) operation

3. Affordability with acceptable performance

The purpose of Multifunction Subarray Radar (MFSAR) is to fulfill a variety of different tasks. Generally the cost is proportional to the number of radiating and control elements, as well the complexity of construction and maintenance. For a modern high performance radar antenna, the basic acceptable antenna parameters are the following [Ref. 2]:

Antenna gains: 30 dB (minimum)

Target tracking accuracy: 5 mrad

Azimuth beam steering: $\pm 45^{\circ}$ (Azimuth)

Azimuth/elevation coverage: $360^{\circ}/ 60^{\circ}$

Peak sidelobe level: -45 dB

B. PREVIOUS APPROACHES

There are two basic approaches that have been considered as a solution for a wideband multifunction system from the standpoint of the array aperture. The first is a segmented approach, where each segment or component is dedicated to a separate system and bandwidth. A segmented aperture provides better performance for each individual function by separating the size and position of the antenna. The second approach, a shared aperture, however, provides multiple frequency operation in the same aperture. Generally the performance at a single frequency is not optimum.

The proliferation of advanced sensor and communication systems onboard military platforms has led to a multitude of systems. A U.S Navy Aegis cruiser, for instance, has over 100 antennas and the number is expected to rise as new systems are added [Ref. 3]. A reduction of the number of antennas is possible using the shared aperture concept.

Ideally a shared aperture of the type used on ships should operate over a wide bandwidth, for example, 10 MHz to 10 GHz (three decades). If the aperture is shared by separate narrow band systems, then the antenna does not have to operate over the complete continuous range of frequencies, but only at the operating "sub-bands" of the component systems. These types of antennas are referred to as multi-band. An example is the Multifunction Electronically Scanned Adaptive Radar (MESAR) [Ref. 4] that employs a dual frequency antenna. The work in MESAR MFAR programs, which began in 1977, showed significant advantages for a radar operating at dual optimal frequencies. This study led to the selection of 1 and 10 GHZ for operating frequencies used for surveillance and tracking functions. The aperture is comprised of two sets of antenna elements, an open-ended waveguide and a dipole, for the low and high frequency bands, respectively. The proposed system will therefore perform these important radar functions at maximum efficiency.

C. MULTIFUNCTION SUBARRAY RADAR

Modern phased array radars are used in a multifunction fashion, with the required functions being search, tracking and fire control. A major impetus of using MFSAR is cost reduction. For example, if phase control is at the subarray level and each subarray is formed by 5x5 elements, then the total number of transmit/receive modules is reduced by a factor of 25 for contiguous subarrays. With widely spaced subarrays, not is there a savings in control elements, but also higher resolution. When the subarrays are widely distributed the potential resolution increases significantly. The disadvantage is the occurrence of grating lobes if the subarrays are widely spaced compared to the wavelength. The features of MFSAR are summarized in the following sections.

1. Advantages of MFSAR

The major advantages of using multifunction subarray radar are the following:

- More efficient scheduling of the track and search functions compared to separate systems (track-while-scan, TWS capability).
- Rapid steering of the beam to the desired direction as needed.
- Formation of search and track beams with maximum flexibility.
- Savings in the number of control elements and decrease in the complexity of digital beamforming.
- Increase in the angular resolution by distributing subarrays along the superstructure of vessel.

2. Disadvantages of MFSAR

The major disadvantages of using multifunction subarray radar are the following:

- Compromise in the performance of individual functions to obtain an optimum balance in the component tasks.
- Extra grating lobes introduced by large subarray spacing.
- Low beam efficiency from the presence of grating lobes.

D. SCOPE AND ORGANIZATION

1. Scope

In this research, some methods of correcting the above disadvantages are examined. The grating lobe problem is severe for subarray spacing over a wavelength. However, it is possible to suppress the grating lobes through control of the subarray factor. In other words, the nulls of the subarray pattern are placed at angles where the grating lobes occur. There is a limit to the effectiveness of this method, as the gaps between subarrays get larger. Some additional improvement is achieved if separate transmit and receive antennas are used, and grating lobes are allowed for only one of the two antennas. For example, if the transmit antenna has grating lobes, then the receive antenna will not. Furthermore, the nulls of the receive antenna can be placed at transmit antenna grating lobe locations. Consequently the two-way gain pattern will have no grating lobes.

An additional improvement may be possible with digital arrays that have amplitude control at each element. The transmit array factor and subarray factor, as well as the receive array, can be phase and amplitude weighted to give low sidelobe performance.

This thesis demonstrates that distributed antennas of MFSAR can provide better performance with fewer elements than the conventional MFAR by using separated subarrays.

2. Primary Research Question

There are two related research questions addressed in this research:

a) how to increase the angular resolution of shipboard radar through wideband distributed subarray antennas, and

b) how to suppress the grating lobes in the pattern of widely spaced subarrays by design of the subarray pattern or design of a two-way pattern.

3. Organization

Chapter II provides an overview of the array theory that is used in this thesis. A definition of the array factor (AF) is given. Antenna parameters such as beamwidth, directivity, aperture efficiency, grating lobes and pattern scanning, are presented. The assumptions and limitations are introduced.

After a description of various subarray configurations, Chapter III discusses the different methods used in the conceptual design of an MFSAR antenna and the concept of digital beamforming will be discussed in more detail. Some ship design examples are also presented.

Chapter IV provides a summary and conclusions, followed by suggestions for further research into distributed subarray design.

Appendix A provides a glossary of terms and abbreviations used throughout this thesis, and Appendix B provides a listing of MATLAB codes used in the pattern calculations.

THIS PAGE INTENTIONALLY LEFT BLANK

II. SUMMARY OF ARRAY THEORY

This chapter discusses the fundamental theory of phased arrays. The material can be found in most books on antennas, such as [Ref. 5] and [Ref. 6].

A. ARRAY FACTOR (AF)

An array is a collection of smaller, usually identical antenna elements that are excited with complex voltages or currents to obtain a desired radiation pattern. For most applications the elements are arranged in a periodic grid; for example, in two dimensions it could be a rectangular lattice. The array can be divided into smaller groups of elements called subarrays as shown in Figure 2. For simplicity, only a linear array is shown, and the array elements are assumed isotropic.

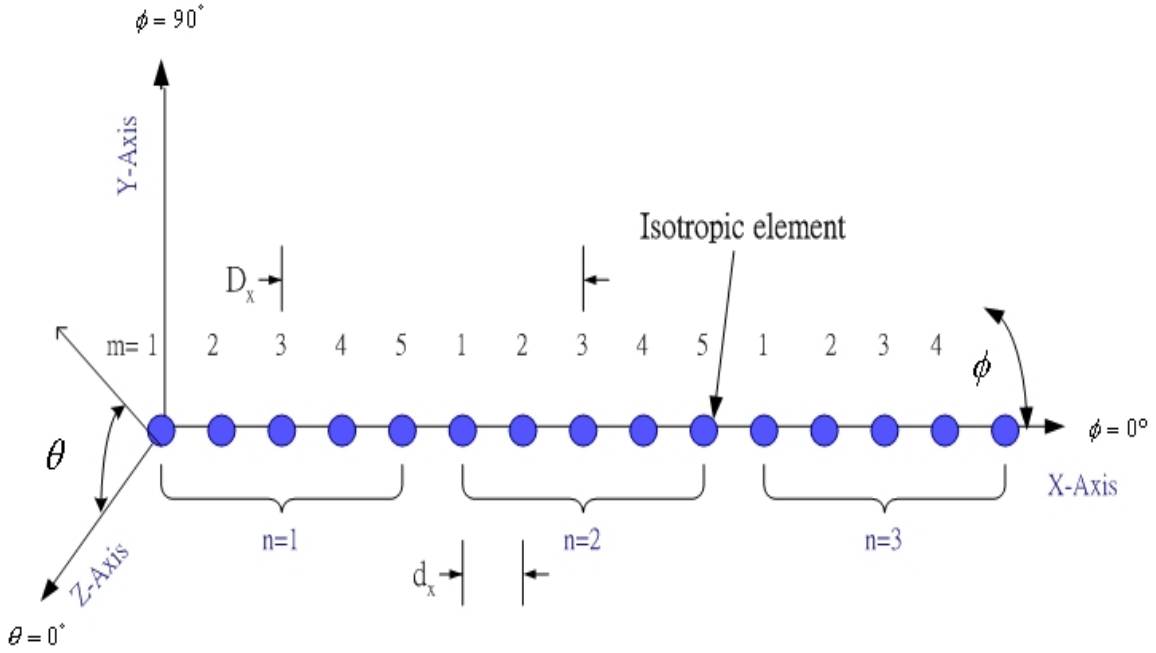

Figure 2. Example of an array of contiguous subarrays, $M = 5$, $N = 3$.

The radiation pattern of an antenna array is the vector sum of the electric field intensity all antenna elements. The array factor for N uniform subarrays, each composed of M isotropic elements along the x-axis is given by

$$\begin{aligned} AF(\theta,\phi) &= \sum_{n=0}^{N-1}\sum_{m=0}^{M-1} I_n J_m e^{jn\frac{2\pi}{\lambda}D_x(u-u_s)} e^{jm\frac{2\pi}{\lambda}d_x(u-u_s)} \\ &= \left[\sum_{m=0}^{M-1} J_m e^{jm\frac{2\pi}{\lambda}d_x(u-u_s)}\right]\left[\sum_{n=0}^{N-1} I_n e^{jn\frac{2\pi}{\lambda}D_x(u-u_s)}\right] \qquad (1) \\ &= AF_s(\theta,\phi)\times AF_c(\theta,\phi), \end{aligned}$$

where

N, M = number of subarrays, number of elements in a subarray

I_n, J_m = subarray, element weights (excitation currents or voltages)

D_x, d_x = subarray center-to-center spacing, element spacing

$u = \sin\theta\cos\phi$, direction cosine in spherical coordinates

$u_s = \sin\theta_s\cos\phi_s$ (θ_s, ϕ_s is the scan direction)

AF_s = subarray pattern determined by the arrangement of elements in a subarray

AF_c = configuration pattern determined by the arrangement of subarrays.

Equation (1) assumes that all subarrays are identical and the elements have uniform spacing. The pattern of the array is then the product of the element factor and the array factor. Isotropic elements have been assumed and, therefore, the element factor (EF) is 1. The use of subarrays allows the array factor to be separated based on the geometry and excitation of subarrays.

B. ANTENNA PARAMETERS

1. Beamwidth Between First Nulls (BWFN)

The beamwidth between the first nulls is defined by the subtended angle of the mainlobe in the antenna pattern. If the element and subarray weights in Equation (1) are assumed unity, then the normalized antenna pattern is given by:

$$\left|AF_{norm}(u)\right|^2 = \left|\frac{\sin(\frac{M\xi}{2})}{M\sin(\frac{\xi}{2})}\frac{\sin(\frac{N\psi}{2})}{N\sin(\frac{\psi}{2})}\right|^2, \qquad (2)$$

where

$$\xi = \frac{2\pi}{\lambda} d_x (u - u_s)$$

$$\psi = \frac{2\pi}{\lambda} D_x (u - u_s).$$

The subscript "norm" denotes the normalized array factor. The BWFN is determined by the first zero of the numerator. Since the phase term of the subarray is changing much faster than the phase of elements ($ND_x \gg Md_x$), the BWFN is determined mainly by the phase of subarrays given by $u - u_s = \pm 1/ND_x$ so $\theta_{BWFN} = 2\sin^{-1}(1/ND_x)$ in the plane $\phi = 0^\circ$. The BWFN, therefore, is determined by the entire aperture size (i.e., the distance between the edges of the two farthest separated subarrays, $L \approx ND_x$).

2. Half Power Beamwidth (HPBW)

The half-power beamwidth of a linear array is defined as the angular separation between two points, one on each side of the main beam maximum, at which the power is reduced by half. The HPBW is determined mainly by the subarray configuration pattern. For a half-wavelength spaced linear array with uniform excitation, the HPBW can be approximated by $\theta_{HPBW} \approx 50.8\lambda / L$ in degrees, where $L \approx ND_x$ is the entire length of the aperture.

3. Directivity and Gain

Directivity is defined as the ratio of the maximum radiation intensity in the main beam to the average radiation intensity [Ref. 7]. For a two-dimensional uniform rectangular array of isotropic elements, the directivity can be approximated by $D = 4\pi\eta L_x L_y \cos\theta_s / \lambda^2$, where η is the aperture efficiency, L_x, L_y are the dimensions of the array in the x, y directions, and θ_s is the scan direction. This approximation is good as long as there are no grating lobes in the visible region. Subsequently it is assumed that there are no other losses other than those due to amplitude tapering. In this case the directivity and gain are equal.

4. Aperture Efficiency

Aperture efficiency is a measure of how efficiently the antenna physical area is utilized. If the element or subarray amplitudes are not equal, the aperture efficiency is given by the taper efficiency. For a planar array in the $x - y$ plane

$$\eta = \frac{\left| \sum_{n=1}^{N_x} \sum_{m=1}^{N_y} I_{mn} \right|^2}{N_x N_y \sum_{n=1}^{N_x} \sum_{m=1}^{N_y} \left| I_{mn} \right|^2}, \tag{3}$$

where N_x and N_y are the number of elements in the x and y directions, respectively, and I_{mn} is the amplitude of the mn th element weight. The weighting can be applied to either the AF_c or AF_s summation.

5. Grating Lobes

Grating lobes occur when more than one period of the array factor appears in the visible region ($\pm 90^\circ$); when either the element or subarray spacing in the Equation (1) is more than one wavelength. For MFAR it is likely the subarray spacing is larger than one wavelength, and thus grating lobes will exist, as shown in Figure 3. In theory, the grating lobes could be suppressed by using either unequally sized or randomly spaced subarrays, at the expense of higher complexity, average sidelobe level increase, and difficulties in applying ADBF [Ref. 8]. Another possible means of suppressing grating lobes is to use

two separate antennas for transmit and receive (i.e., a quasi-monostatic radar). The two-way gain $G_t G_r$ occurs in the radar range equation for the signal-to-noise ratio (SNR)

$$SNR = \frac{P_r}{N} = \frac{P_t G_t G_r \lambda^2 \sigma}{(4\pi)^3 R^4 K T_s B_n}, \tag{4}$$

where P_r is the received target signal, P_t is the transmit power, σ the target RCS, λ the wavelength and R the range. The product KT_sB_n is the noise power, K is Boltzmann constant, T_s system noise temperature and B_n radar bandwidth. Grating lobes can be allowed in the receive pattern and then eliminated by placing transmit nulls in those directions. The cost is usually a reduction in transmit antenna efficiency.

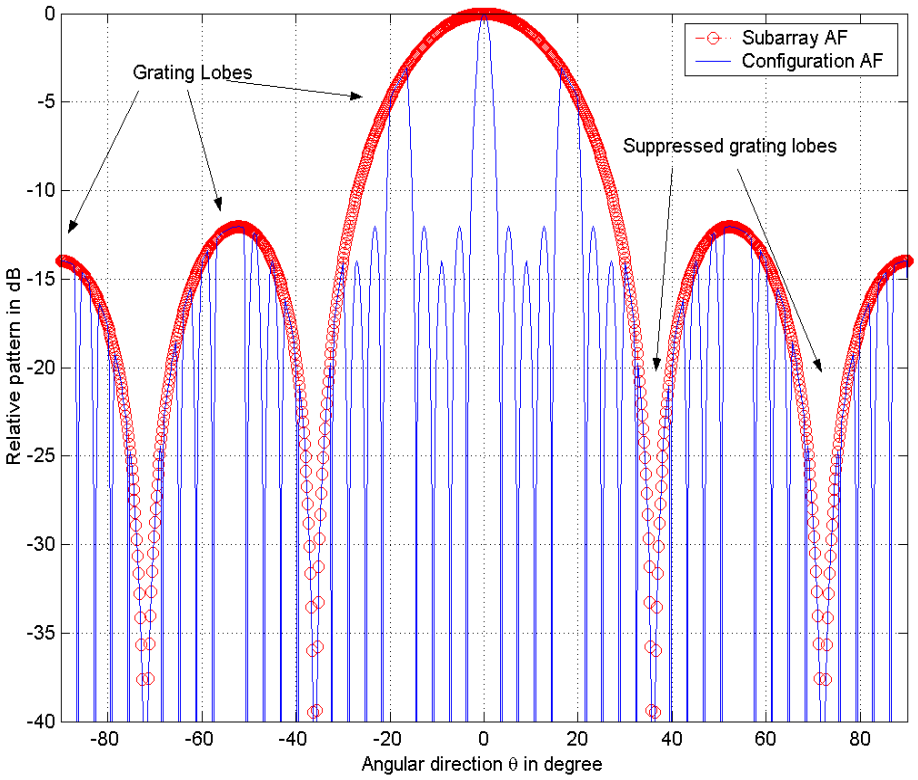

Figure 3. Grating lobes produced by subarrays $D_x = 5\lambda$ $\left(d_x = 0.5\lambda, N = 5, M = 5\right)$.

6. Electronic Scanning

Electronic scanning is defined as a method of positioning a beam with the antenna aperture remaining fixed. The basic electronic scanning techniques are phase shifting, true time delay, frequency scanning, and feed switching. Some possible control configurations for beamforming are shown in Figures 4 through 6. To avoid the problems of beam squinting and broadening that occur over wide frequency bands, it is desirable to have true time delay at each element. This is difficult to achieve using conventional microwave beamforming. However, it has been accomplished using photonic devices (optical fiber) and through signal processing in digital antennas. Subsequently, true time delay is assumed at each element.

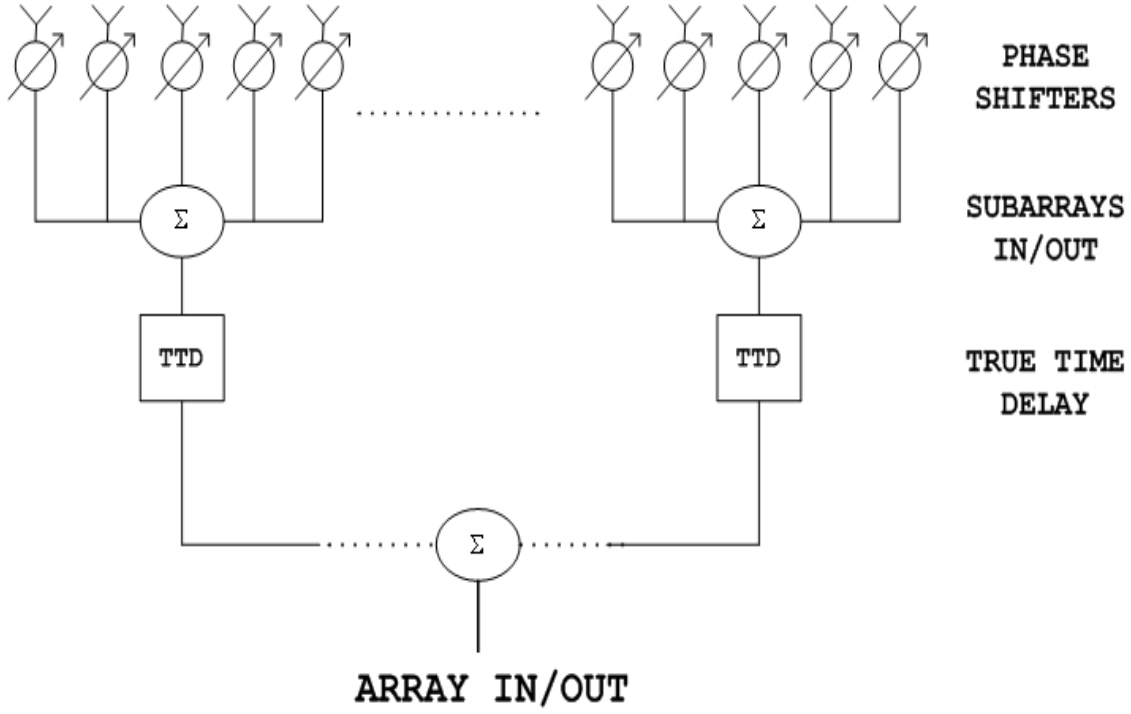

Figure 4. True time delay at the subarray level with phase shifters at the element level.

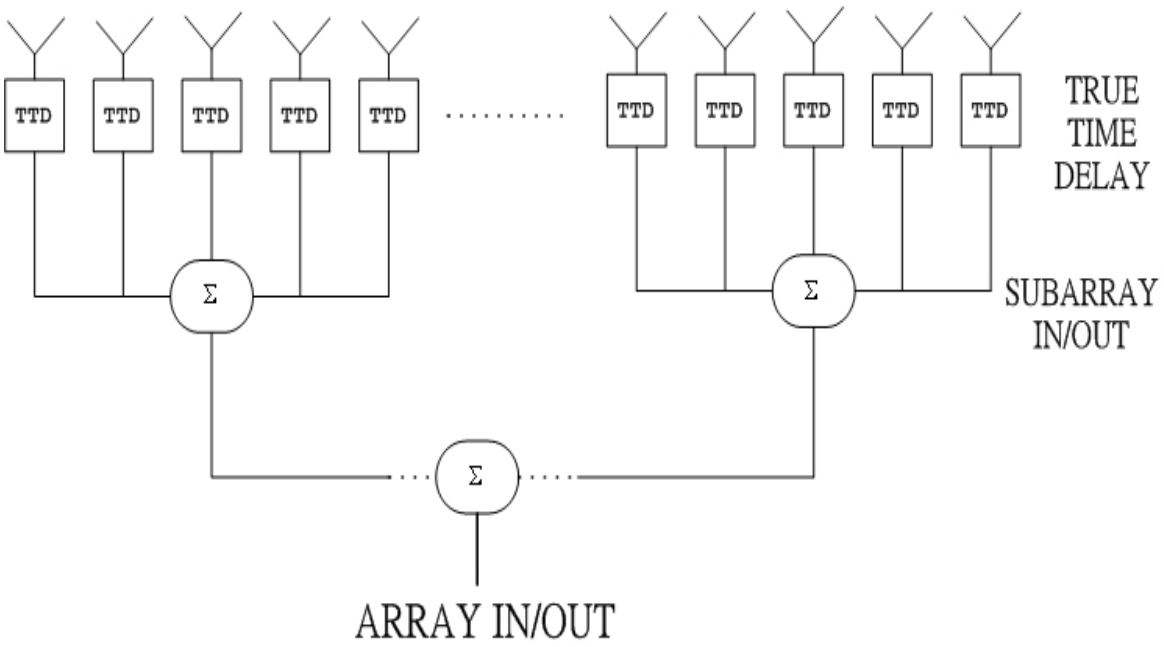

Figure 5. True time delay at the element level.

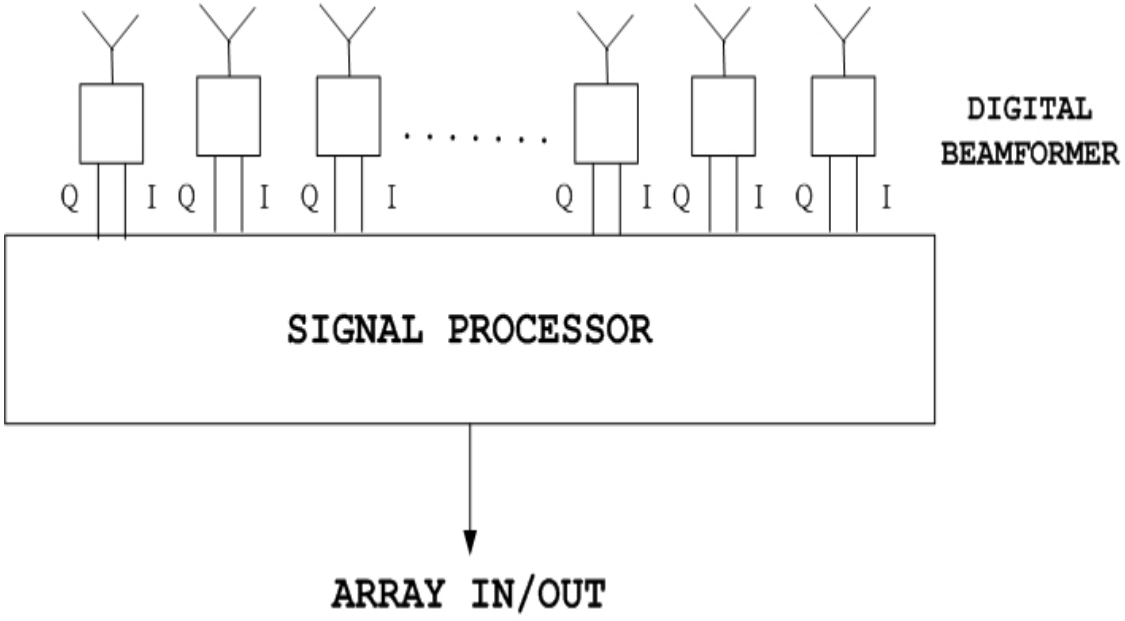

Figure 6. Digital beamforming.

C. RADAR SYSTEM CONSIDERATIONS

The radar range equation (4) gives the fundamental relationship between radar design parameters. A main objective of this thesis is to propose a possible conceptual design of distributed subarray antennas, using separate transmitter and receiver antennas, which is a form of quasi-monostatic radar.

1. Maximum Detection Range

From Equation (4), the maximum detection range of the radar for a given signal-to-noise ratio can be rewritten as

$$R_{\max}{}^4 = \frac{P_t G_t G_r \lambda^2 \sigma}{(4\pi)^3 (SNR)_n K T_s B_n} = \frac{P_t G_t A_{er} \sigma}{(4\pi)^2 K T_s B_n (SNR)_n}$$
$$= \frac{P_{avg} G_t A_{er} \sigma}{(4\pi)^2 K T_s F_n (B\tau) f_p (SNR)_n}, \qquad (5)$$

where

P_{avg} = average transmitter power

A_{er} = receiver effective aperture area

F_n = receiver noise figure

B = receiver bandwidth

τ = pulse width

f_p = pulse repetition frequency

$(SNR)_n$ = minimum signal-to-noise ratio after n -pulses are integrated.

This equation illustrates several important tradeoffs in the design of radar

(1) Power-aperture product: One of the most important measures of the capability of long-range surveillance radar is the product of average power and effective aperture size $(P_{avg} A_{er})$, which controls the amount of power transmitted by the aperture. If the aperture size could be larger, the average power required for detecting the target at a given range would be decreased when all other factors are constant.

(2) Frequency dependence: Although the frequency does not appear explicitly, it is easier to achieve high power at low frequencies because high voltages are applied to larger distances and breakdown can be avoided. Furthermore, atmospheric loss is less at lower frequencies.

2. Angular and Range Accuracy

Range and angular resolution provide improved accuracy, since accuracy is inversely proportional to signal bandwidth and directly proportional to beamwidth as [Ref. 9]

$$\sigma_{\varepsilon} = \frac{\theta_{HPBW}}{K_g \sqrt{2SNR_n}}, \tag{6}$$

where

σ_{ε} = angular accuracy

θ_{HPBW} = antenna beamwidth

K_g = gradient of the difference beam in the monopulse antenna configuration.

Once again, the angular accuracy is proportional to the beamwidth θ_{HPBW} and inversely proportional to square root of SNR in this equation.

Since the range resolution is $\Delta R = c\tau/2 = c/2B$ [Ref. 3], the range accuracy is improved by having a wide instantaneous bandwidth.

D. SUMMARY

This chapter has presented the basic theory of arrays and discussed some fundamental radar system design tradeoffs. This research is primarily concerned with increasing radar resolution by an increase in the antenna aperture. Because large unobstructed smooth surfaces are limited on ships and aircraft, it is necessary to construct large arrays by combining signals from distributed subarrays. Unfortunately, this results in grating lobes.

In order to suppress the grating lobes the subarray sizes, locations and excitations can be adjusted. Furthermore, separate transmit and receive antennas can be employed, and designed so that the two-way pattern has suppressed grating lobes. These last two approaches are examined in subsequent chapters. To simplify the analysis the following assumptions are made:

1. The element factor is neglected,
2. Generally, a linear array is used with x being the array axis,
3. The antenna is at the center of a spherical coordinate system, where the $x-y$ plane is the earth's surface and z the zenith direction,
4. Mutual coupling is neglected, and
5. A constant frequency or time-harmonic wave is assumed (e^{jwt} time dependence), and therefore phaser quantities appear in the equations.

III. DISTRIBUTED SUBARRAY ANTENNA

A. SUBARRAY METHODS AND CONFIGURATIONS

The concept of subarraying arises from the requirement of modern radar for high resolution. When the targets to be tracked have very small RCS, and the radar must have fine angle resolution to track multiple closely spaced targets, the antenna apertures have to be electrically large.[1] Because of the large number of array elements required, grouping of elements to reduce the beamforming complexity and control cost is inevitable. The subarrays can be divided into several types as shown in Figure 7. They are discussed in the following section.

1. Subarray Configurations

In terms of control there are generally four types of subarray configurations, as shown in Figure 7:

1) Amplitude and phase control at each element (Figure 7(a)) — this allows complete control of both AF_s and AF_c,
2) Phase only control at each element (Figure 7(b)) — this allows scanning of both AF_c and AF_s,
3) Amplitude and phase control of the subarray pattern AF_c (Figure 7(c)) and
4) Amplitude and phase control of the array factor AF_c (Figure 7(d)).

[1] Synthetic aperture radar (SAR) is another solution to the resolution problem, but it has its own disadvantages and limitations [Ref. 10].

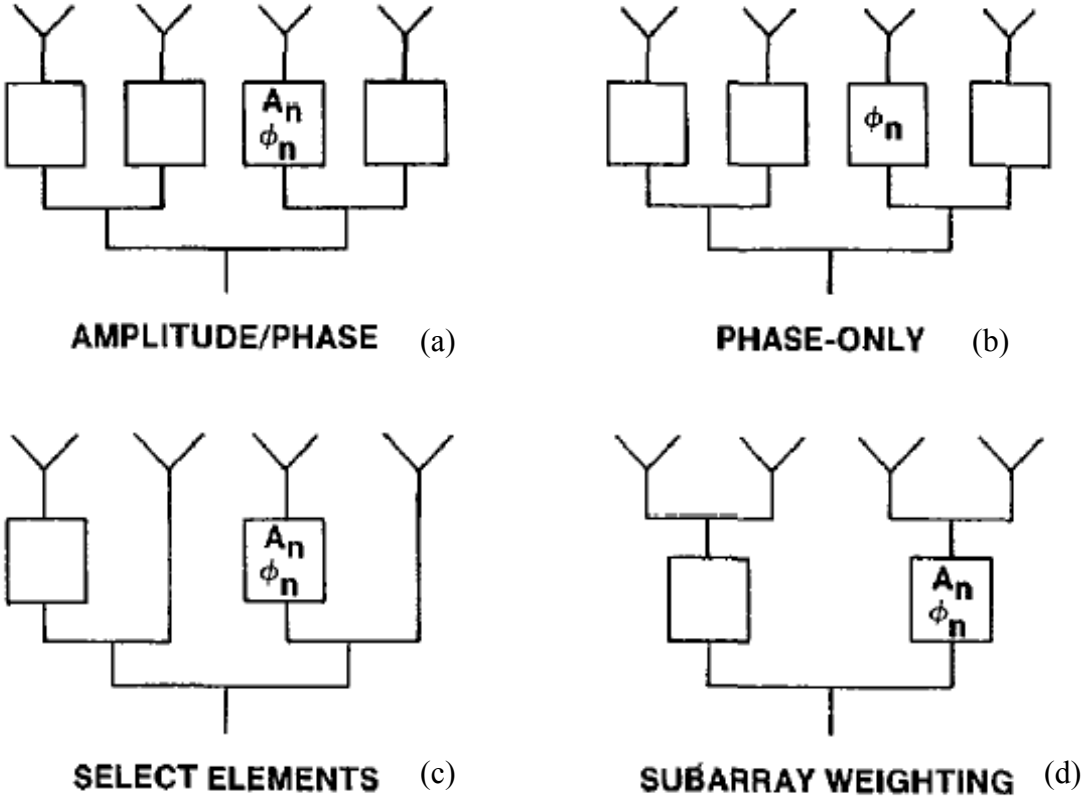

Figure 7. Typical subarray control configuration [From Ref. 11]

Amplitude and phase control at each element is undoubtedly the most costly but also the most desired in terms of beam pointing and sidelobe level (SLL). The second alternative is to control element phase only, which is very attractive since in a conventional phased array the required controls are available at no extra cost. However, the grating lobes in the DSA approach severely distort the pattern, and a phase-only correction is not very effective. In this thesis, it is assumed that complex weights can be applied at both the element level and the subarray level. Furthermore, the weights have true time delay behavior.[2]

[2] As a practical matter, if complex weights can be applied at the element level, then there is no need for weighting at the subarray level.

2. Basic Properties of DSA Pattern

Due to the large spacing between subarrays in a periodic DSA, there are many grating lobes in the visible region. For example, if the spacing between subarrays is 5 wavelengths, there will be 10 grating lobes in the $[-\pi/2, \pi/2]$ visible region, that are located at the angles $\sin^{-1}(\pm p/5)$ radians ($p = 1, 2, 3, \cdots$) as shown in Figure 3. The following are some basic characteristics of the periodic subarray configuration:

- The array pattern of identical periodic subarrays can be separated as a multiplication of a subarray factor (AF_s) and the subarray geometry and excitation factor (AF_c) as shown previously in Equation (1),
- The number and the intensity level of sidelobes between two adjacent grating lobes are dependent on the number and position of the subarrays. Similar to the uniform linear array, there will be $N-2$ sidelobes with a peak intensity level about –13 dB in the unity weighting case, and
- The number of subarrays does not have any effect on the number of the grating lobes as long as subarrays are spaced approximately equal. The intensity level of the sidelobes is decreased with an increase in the number of subarrays. This implies that having multiple small subarrays that are spaced uniformly gives better performance in both SLL and grating lobes than having two large subarrays spaced far apart.

3. Methods for DSA Pattern Design

There are two approaches to reducing grating lobes. The first is based on pattern multiplication, as illustrated in Equation (1). The grating lobes in one factor can be suppressed by placing nulls of the other factor coincident with the grating lobes. The key to this approach is that the grating lobes and nulls are periodic in arrangement. A second approach to reducing grating lobes is to use an irregular spacing or unequal sized subarrays, thereby reducing the peak grating lobes by redistributing the energy into the sidelobe regions.

The process of pattern design can be divided into two stages. The first stage is to lower the SLL and eliminate the grating lobes as much as possible by synthesis of the appropriate AF_c and AF_s functions. For the subarray spacings of interest the first pair of grating lobes (one on either side of the main lobe) are not easy to suppress because of their narrow width and close proximity to the main lobe. The second step is to suppress the remaining grating lobes by either a high contrast (i.e., low sidelobes relative to the mainlobe) transmit pattern or by specific placement of the nulls in the transmit pattern.

There are several simple methods used in the pattern synthesis of DSA in this thesis. The process of direct nulling by pattern synthesis is discussed next.

a. Pattern Multiplication Principle

Since the antenna is composed of periodic subarrays with the same spacing, their pattern could be predicted from Equation (1) and the null locations manipulated. The angular directions of grating lobes in the configuration pattern AF_c are given by

$$u = u_s \pm \frac{p\lambda}{D_x}, \tag{7}$$

where p is a non-zero integer. The nulls of the uniform subarray pattern AF_s are located at

$$u = u_s \pm \frac{p\lambda}{Md_x}. \tag{8}$$

The condition for suppressing grating lobes is $D_x / d_x = M$. Unfortunately this is exactly the condition of contiguous subarray, which contradicts our DSA approach. Since the nulls of the uniform subarray pattern are located in $2\pi / M$ angular increments, if the element number M is chosen correctly, some ratio of grating lobes in the configuration pattern will be suppressed. For example, if $D_x / d_x = 5\lambda / 0.5\lambda$, and let $M = 5$, the even integer numbers of grating lobes will be suppressed as shown in Figure 8 (a).

This only solves half of the problem. The two-way pattern synthesis gives additional freedom to use the nulls of the transmit pattern to suppress the remaining grating lobes in the receive pattern. The two-way pattern is defined as

$$AF_{2way} = AF_{Tx} \times AF_{Rx} = AF_{Tx} \times AF_s \times AF_c \,. \tag{9}$$

For example, the receive pattern of 16 weighted subarrays, and transmit pattern of 20 weighted elements, spaced in 0.5λ is shown in Figure 9. In this example the transmit antenna has a Chebyshev distribution.

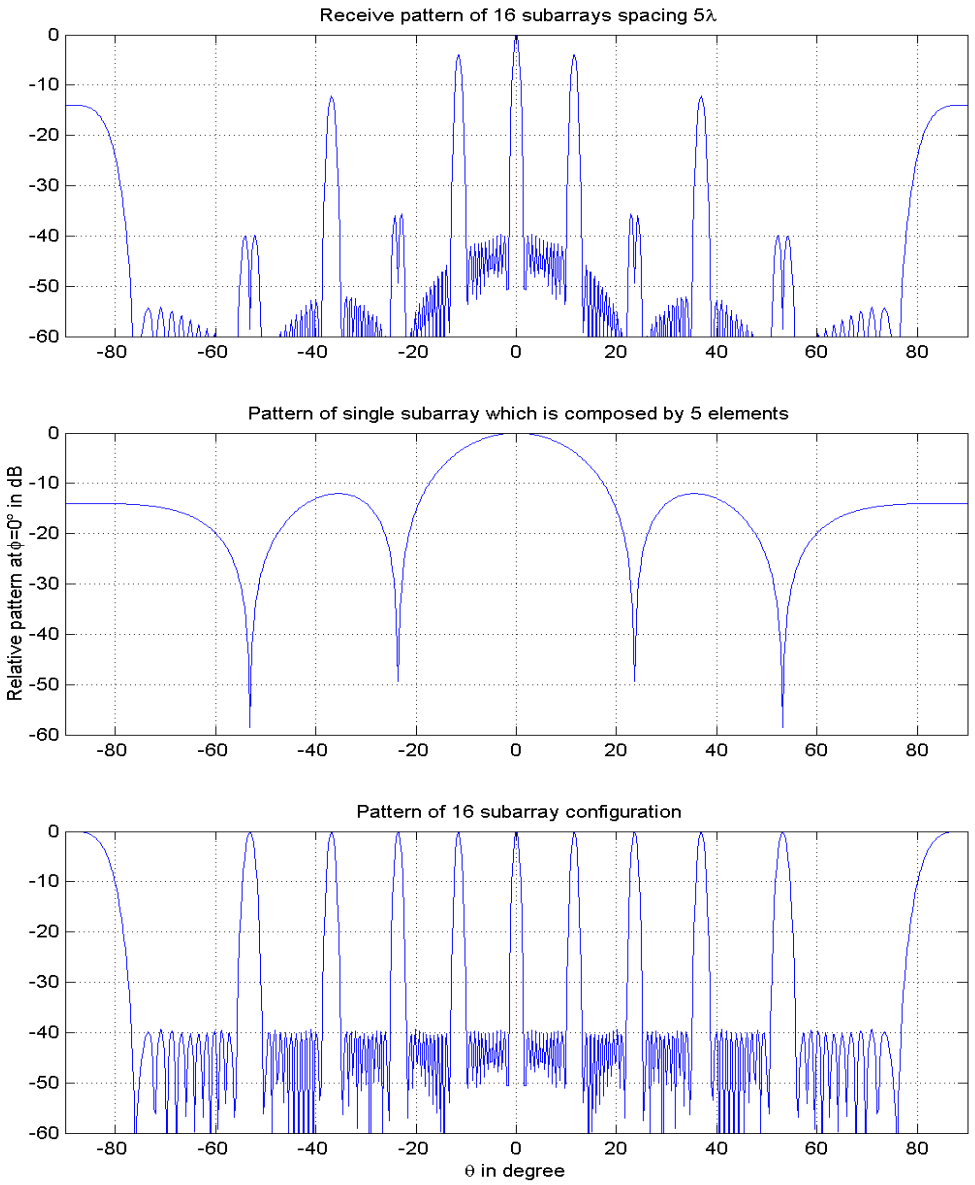

Figure 8. The grating lobes suppressed by 5 element subarrays pattern, (a) total receive array pattern, (b) subarray factor AF_s , and (c) subarray configuration factor AF_c .

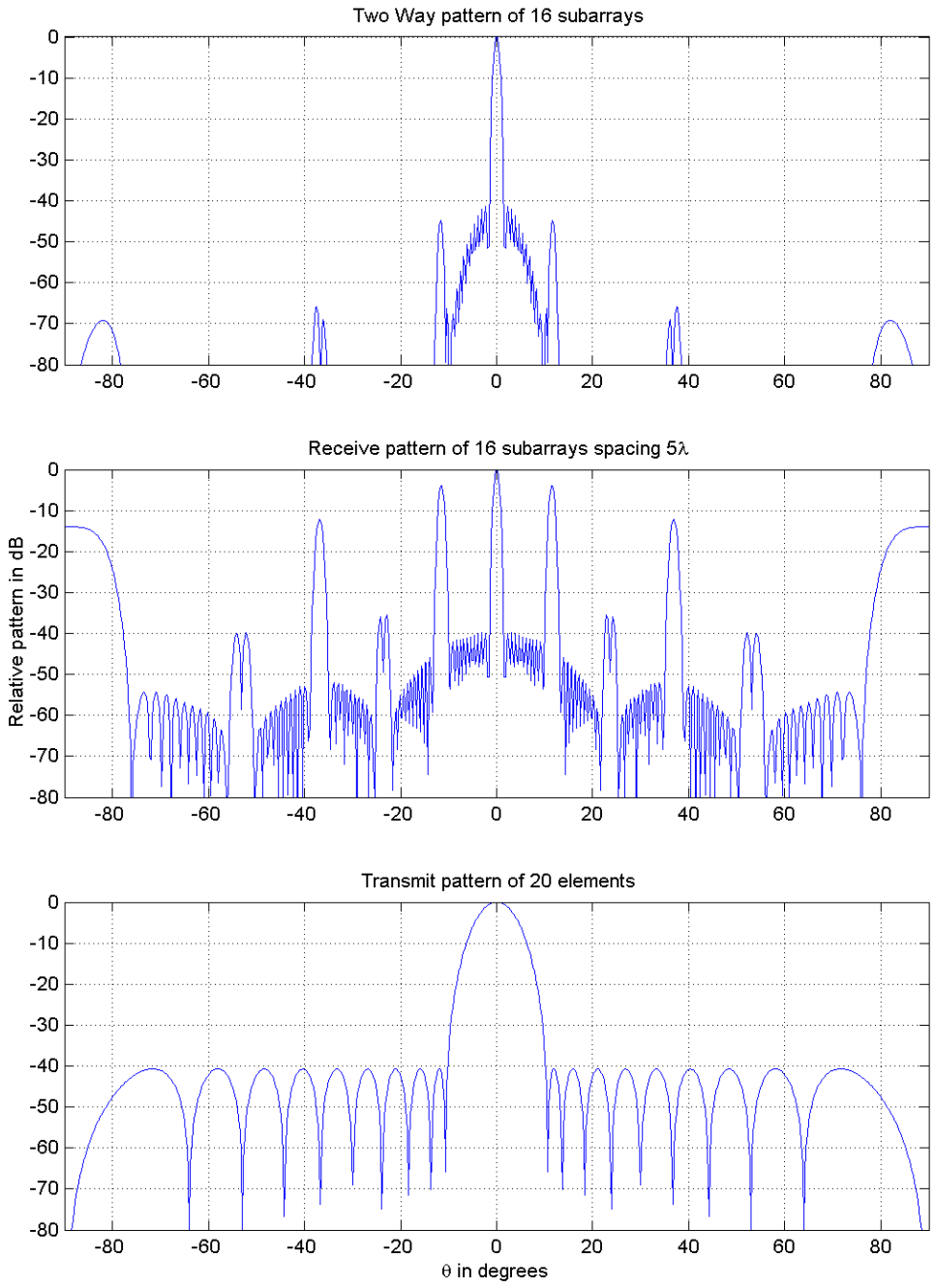

Figure 9. Example of pattern multiplication principle (a) two-way pattern AF_{2way}, (b) receive pattern AF_{Rx}, (c) transmit pattern AF_{Tx}.

b. Modified Minimax Algorithm to Find the Geometry of Lowest Sidelobes by Perturbation of Subarray Location

There are many different approaches to the design of low sidelobe patterns in phased array systems. Since the goal of the first step is to minimize the sidelobes and grating lobes, one such approach is to displace the subarray locations based on the Dolph-Chebyshev theorem [Ref. 12].

Every subarray considered is identical (same AF_s) and has symmetric weights about the center of the array. The AF_c can be represented as

$$AF_c(u) = \sum_{k=0}^{K-1} \alpha_k \cos(\frac{2\pi D_k}{\lambda} u)\ ,\ 0 \le u = \sin\theta \le 1, \tag{10}$$

where

$K = \frac{N}{2}$ when N even, $\frac{N+1}{2}$ when N odd, N is the number of subarrays and

D_k = distance between the *k*th subarray and *0*th subarray.

For odd length arrays the weights to be applied on the individual subarrays are found from $I_0 = \alpha_0$, $I_n = I_{-n} = \alpha_n / 2$ and in the even case $I_n = I_{-n} = \alpha_n / 2$.

By fixing the location of the center and edge subarrays, the lower bound on the beamwidth of the main lobe of AF_c is approximately $u_0 \approx 0.886\lambda / L$ where L is the length of aperture, as the initial guess. The Minimax algorithm is used by setting the lower and upper bound for location of other subarrays, and the obtaining subarray-optimized positions by minimaxing the Chebyshev basis function in the region $u_0 \le u \le 1$.

The application of this method to the 16 uniform subarrays of 5 uniform elements each is shown in Figure 10. Compared to the original receive pattern of 16 Hamming-weighted subarrays with equal spacing in Figure 8(a), although the peak grating sidelobes are decreased from 4 dB to 11 dB, the average sidelobe level becomes much higher because of the perturbation in locations. Also note that the narrow beamwidth is similar to the uniform weighted subarray. The locations of the subarrays in wavelengths are D_n = [0 2.5000 11.6208 15.1714 19.2073 24.6143 29.2136 35.0000 40.0000 45.7864 50.3857 55.7927 59.8286 63.3792 72.5000 75.0000].

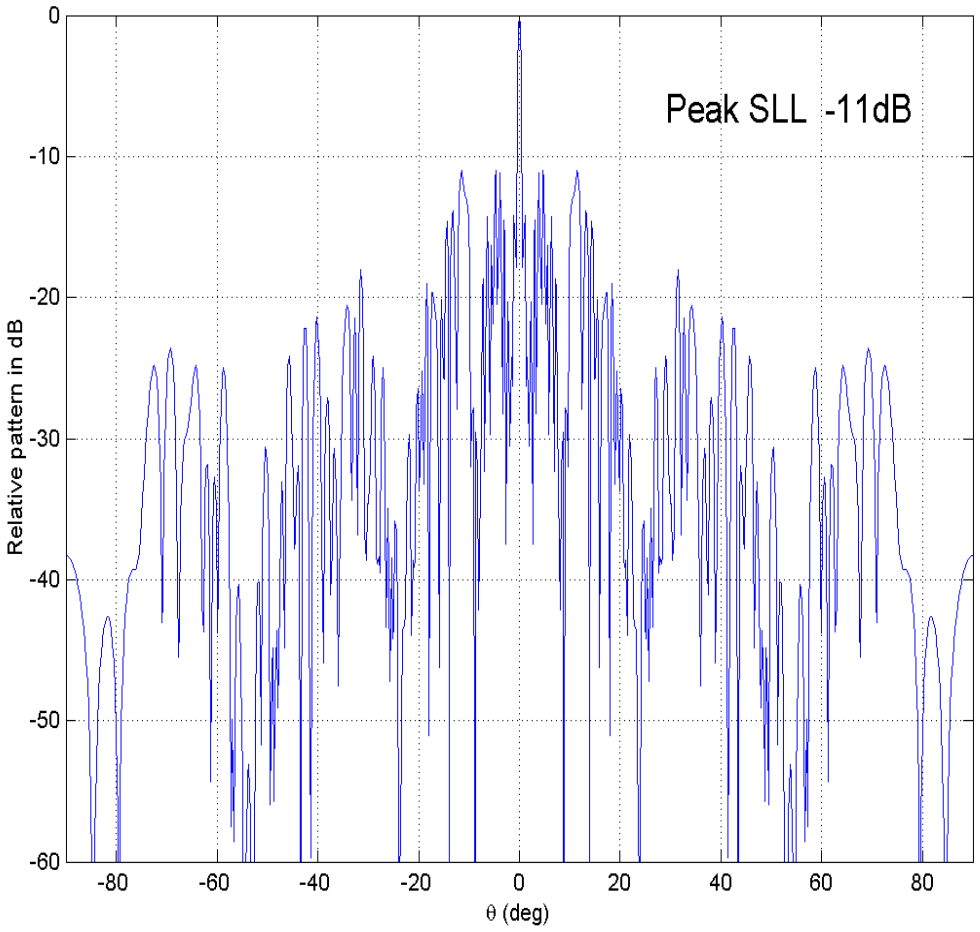

Figure 10. One-way array pattern of 16 location-perturbed uniform subarrays

The same Minimax algorithm can also be extended to synthesis of the weights of the desired transmit pattern. It will find the suitable weights of the transmit elements for selective nulling angles and the specified sidelobe level, which match the grating angles in the receive pattern. The objective function becomes [Ref. 13]

$$\min\{\max_u |W(u_k)(D(u_k) - P(u_k))|\} = \delta \tag{11}$$

where

$u = \pi \sin\theta$, the set of spatial frequencies the response is optimized

W = the error weighting

D = the desired response (intensity level)

δ = deviation between the pattern and desired response

$$P(u_k) = \sum_{k=0}^{K} \alpha_k \cos(\xi_k u),\ \xi_k = \frac{2D_k}{\lambda}.$$

This theorem could be formulated as a matrix equation $\mathrm{A}\vec{\alpha} = D$ where

$$\mathrm{A} = \begin{bmatrix} \cos\xi_0 u_0 & \cdots & \cos\xi_K u_0 & \dfrac{\delta}{W(u_0)} \\ \cos\xi_0 u_1 & \cdots & \cos\xi_K u_1 & \dfrac{-\delta}{W(u_1)} \\ \vdots & \cdots & \vdots & \vdots \\ \cos\xi_0 u_{K+1} & \cdots & \cos\xi_K u_{K+1} & \dfrac{(-1)^{K+1}\delta}{W(u_{K+1})} \end{bmatrix}$$

$$\vec{\alpha} = \begin{bmatrix} \alpha_0 & \alpha_1 & \cdots & \alpha_K & \delta \end{bmatrix}^T$$

$$D = \begin{bmatrix} D(u_0) & D(u_1) & \cdots & D(u_K) & D(u_{K+1}) \end{bmatrix}^T.$$

The coefficients α_k that form the solution to this system can then be used as the element weights of the transmit array. This approach was tried but the null depths were not always sufficient to suppress the grating lobes.

c. Modified Weighting Method for Distributed Subarray

The conventional weighting distributions can be applied to nonuniformly spaced arrays by sampling the continuous distribution at the appropriate points that correspond to the element locations. The phase-shift of elements for scanning needs to be modified accordingly [Ref. 14].

Let the number of the subarrays be N, the number of array elements in the nth subarray $M(n) = M$ (identical subarrays), the distance between the *n*th and *0*th subarrays are $L(n)$ wavelengths, and θ_k the angle from normal direction of the array. Then the phase-shift of the *m*th element in *n*th subarray is

$$\varphi_{mn} = L(n)\frac{2\pi}{\lambda}\sin\theta_k + m\frac{2\pi}{\lambda}d_x\sin\theta_k . \tag{12}$$

The modified Hamming weighting function for a nonuniform spaced subarray is written as

$$W_H(n) = 0.54 - 0.46\cos[\frac{2\pi l_d(n)}{L_d}], \tag{13}$$

where

$l_d(n) = L(n)/d_x$ *n*th subarray position relative to the element spacing

$L_d = L_x/d_x$ aperture dimension relative to the element spacing.

A similar result could be achieved if this modified weighting method is applied to the elements in all subarrays, which yields a smoother sampled distribution than weighting at the subarray level only. However, the array factor cannot be separated because of different subarray factors AF_s. Also $l_d(n)$ has to be changed to the element relative position $l_d(mn)$ in the aperture to apply the weighting function of Equation (13).

Figure 11 shows the receive pattern of modified Hamming weight application on the elements of the same subarrays. Compared to Figure 9(b), there is more suppression of the grating sidelobes at the angles $\theta = \pm 23°, \pm 53°$, but almost the same level everywhere else. The patterns for weighted subarrays versus weighted elements do not differ too much in beamwidth and sidelobe level. The subarray level control scheme is more desired because of its simplicity.

For reference, Figure 12 shows the pattern of 16 uniform weighted subarrays. The pattern of the Hamming weighted elements or subarrays is "cleaner" in terms of sidelobe level especially in the proximity of the mainlobe. The Hamming pattern has a slightly wider beamwidth.

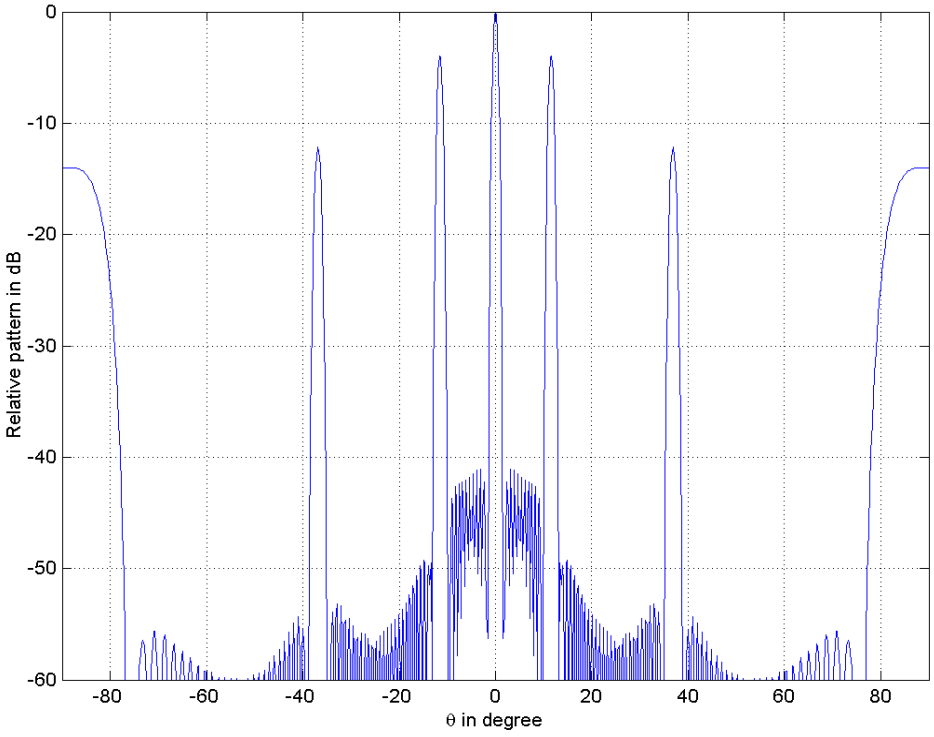

Figure 11. The DSA receive pattern with modified Hamming weights on array elements

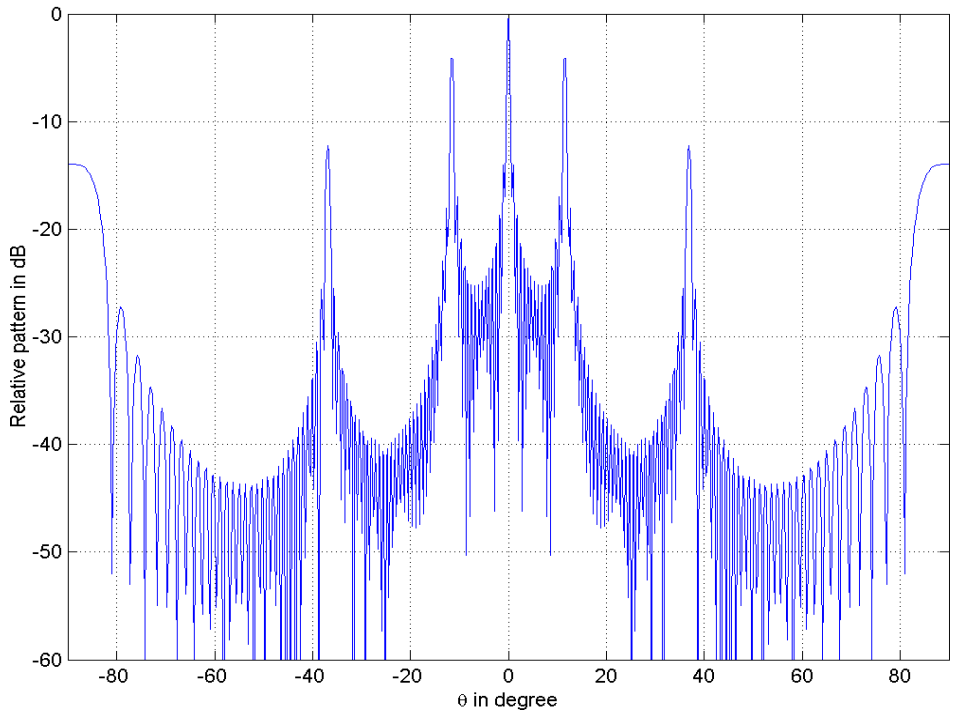

Figure 12. The DSA Receive pattern with uniform weighted subarray elements ($N=16, M=5, D_x=5\lambda, d_x=0.5\lambda$)

d. Equiripple (Parks-McClellan) Design Method of High Contrast Transmit Pattern

Linear antenna arrays are in many ways analogous to one-dimensional digital filters. Restriction of the pattern synthesis problem to that of discrete arrays of finite spatial extent makes the problem similar to that of finite impulse response (FIR) digital filters. When the ideal time delays are used, wideband pattern synthesis reduces to the narrow band case, with each element's delayed waveform receiving a single real weight. In classic narrow band pattern synthesis, an equiripple weighting with narrowest beamwidth for a given sidelobe level was proposed in [Ref. 15].

The Parks-McClellan algorithm is based on an iterative algorithm, which minimizes the maximum amplitude of the ripple (side lobes) present. By the specified angle of the passband (BWFN), stopband (spatial directions outside the mainlobe), frequency response (intensity level) and the maximum deviation from the frequency response the weighted least squares algorithm (WLS) provides an optimal approximation to the desired pattern in the least squares sense. This ensures that the power present in the stopband will be a minimum. The calculation of an array factor of 35 linear elements spaced $\lambda/2$ using MATLAB's built-in Remez function is shown in Figure 13, and the applied weights for each element are shown on Figure 14.

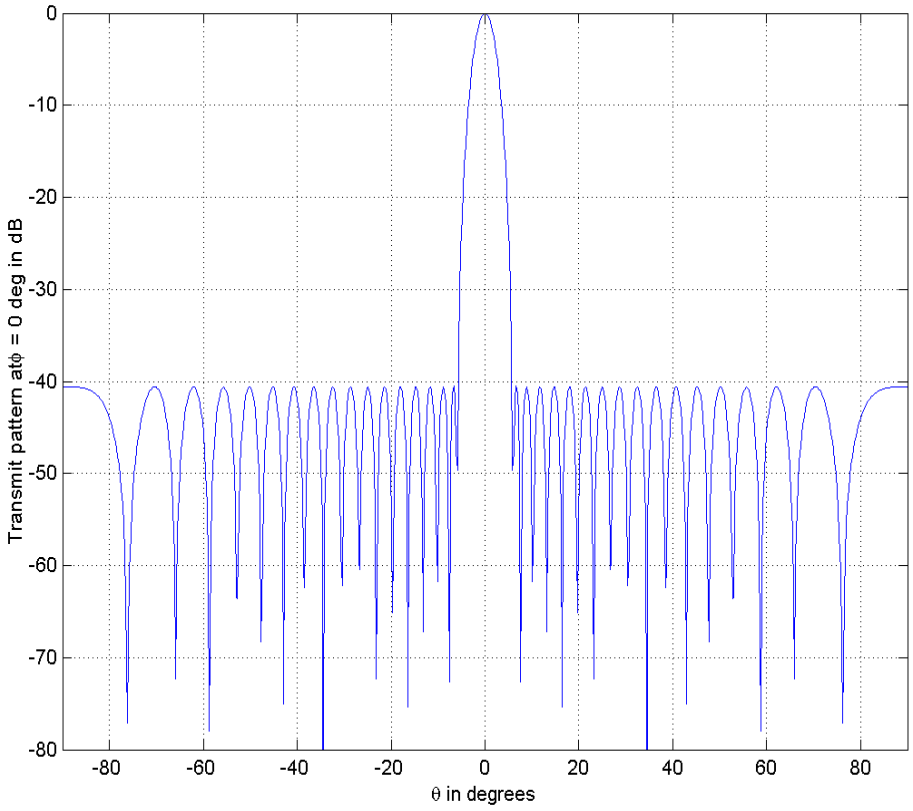

Figure 13. Transmit pattern of 35 equiripple-weighted elements

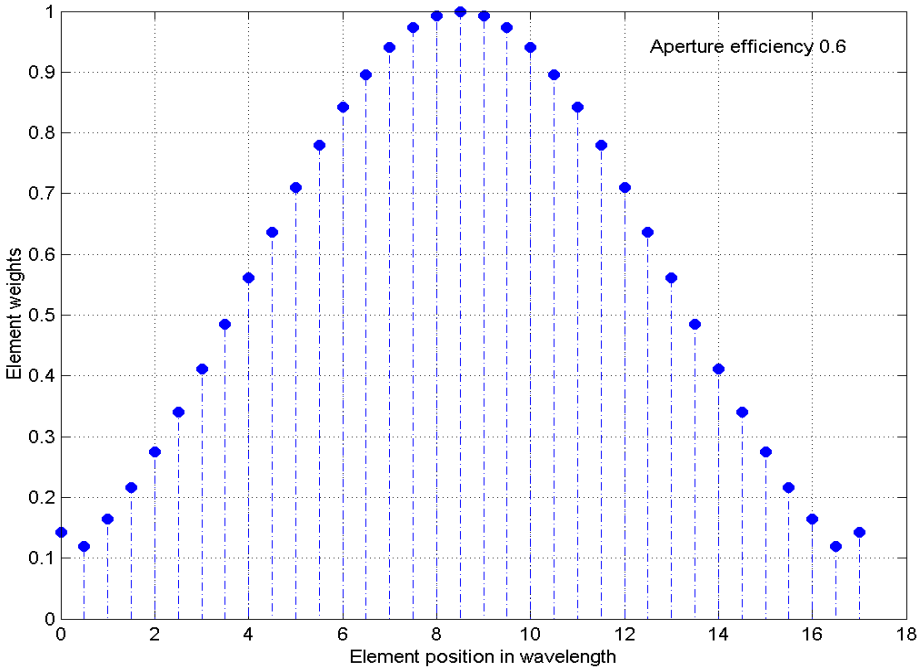

Figure 14. Weights of the transmit elements

B. POSSIBLE SHIPBOARD MFAR DSA DESIGN

There are several reasons why a distributed subarray antenna might be used on a ship. One is the limited surface area available for antenna placement. At low frequencies, the open surface areas are small compared to the wavelength, and narrow beamwidths are not possible with a single contiguous array. By adding more subarrays on other areas of the ship, they can be processed as a DSA resulting in a half power beamwidth of approximately λ / L radians. Any combination of transmit and receive functions could be used. In Figure 15, for example, 1 and 2 transmit only; 3 receives only, etc. This approach can be applied to frequencies where the subarray spacing is in the range of 1 to 5 wavelengths. For an Aegis-sized cruiser this would be in the VHF to UHF frequency regions.

At higher frequencies a DSA might be used to reduce cost and weight. As illustrated in Figure 16 the original aperture size is large enough (in wavelengths) to provide a sufficiently narrow beam, λ / L. Some weight can be eliminated by removing

selected areas of the array, as shown in Figure 17. The thinned areas between the subarrays can be used for other sensors; for example, radar or communication antennas at other frequencies. The penality is grating lobes, although they can be suppressed using the techniques described previously.

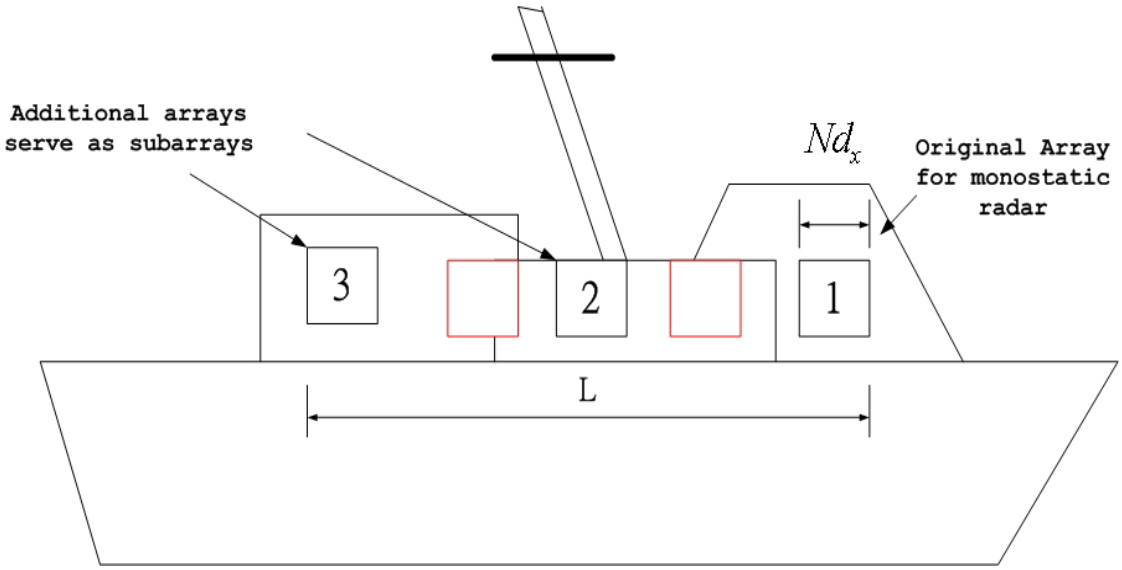

Figure 15. Adding arrays to form a DSA

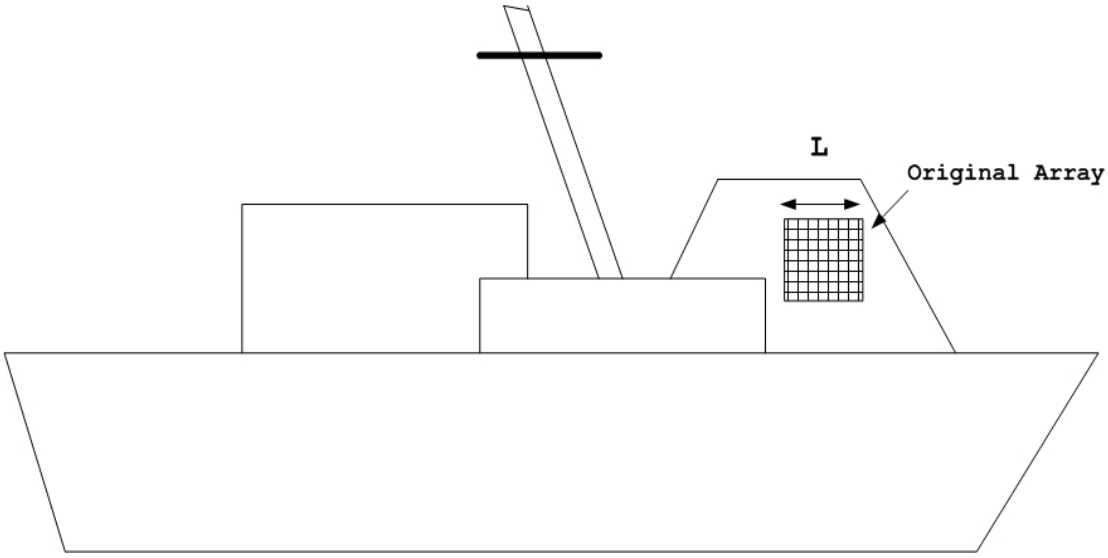

Figure 16. Subarraying applied to a contiguous array

1. MFAR DSA Configuration by Thinning

One possible antenna configuration for a shipboard DSA is shown in the Figure 17. C-band is chosen as the operating frequency for this design. The transmit array is composed of the center 35×35 uniform elements (yellow), which also can be used as part of the receive antenna (blue squares). In theory the transmit pattern could use any number of elements, with the performance improving with the number of elements (narrower transmit beamwidth and higher gain).

The receive antenna uses digital beamforming with 16×8 subarrays, each comprised of 5×5 isotropic elements. Each subarray can have any number of independent functions such as communication, missile guidance, sidelobe cancellation, etc., and they are grouped independently for each function. The following section shows patterns for 16 by 8 subarrays for receive and a continuous 35 by 35 element transmit array.

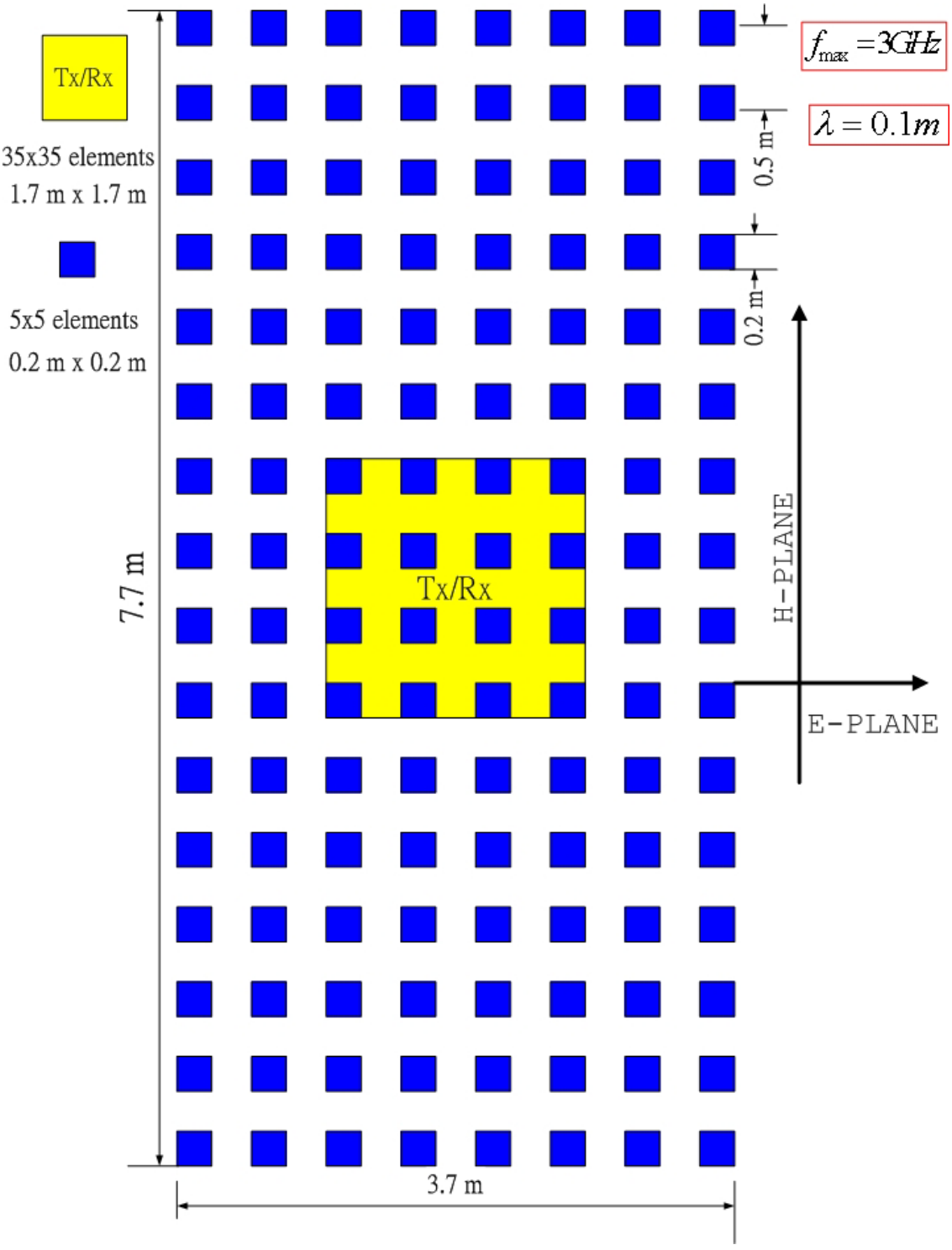

Figure 17. Configuration of MFAR DSA

2. Pattern Synthesis of Shipboard MFAR DSA

Based on the synthesis method introduced on Section A of this chapter, Figure 18 shows the receive pattern from coherent signal processing of 16×8 uniform subarrays. The grating lobes exist at $\theta=11.5°,23°,37°,53°$ (main beam not scanned). By multiplying the transmit pattern of the center 35 elements as shown on Figure 13, the resulting two-way pattern in the H and E-planes is given in Figures 19 and 20. The peak SLL is approximately –45 dB. The grating lobes in the two-way pattern have been reduced to a maximum of –45 dB below the two-way main beam gain. This demonstrates the effectiveness of the 2-way pattern approach.

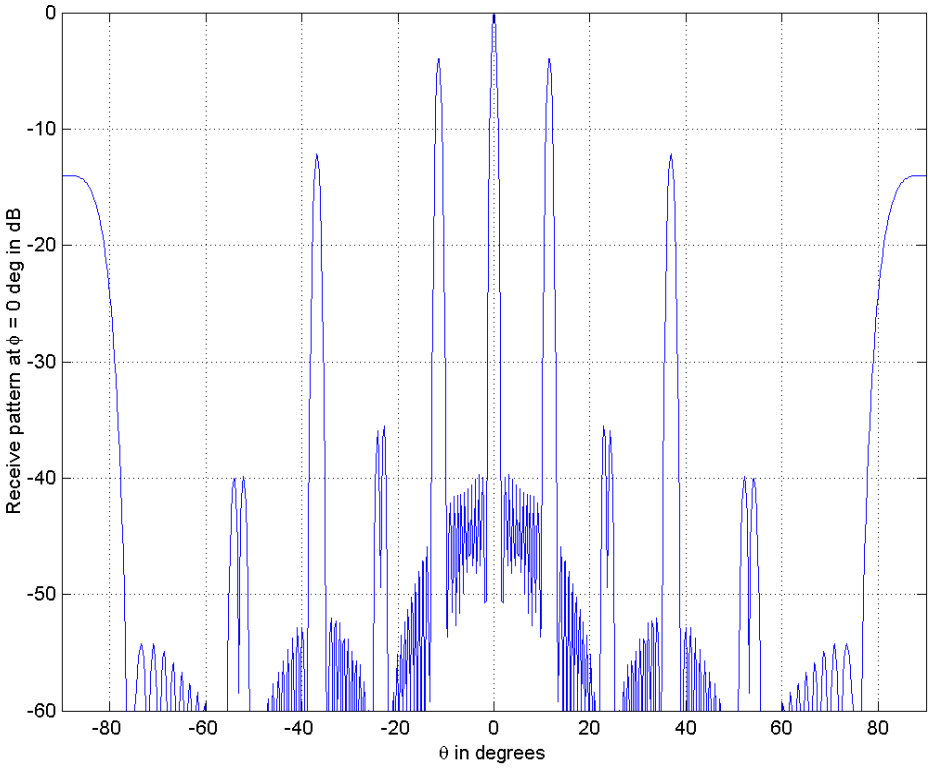

Figure 18. Receive H-plane pattern of 16 Hamming weighted subarrays spaced 5λ

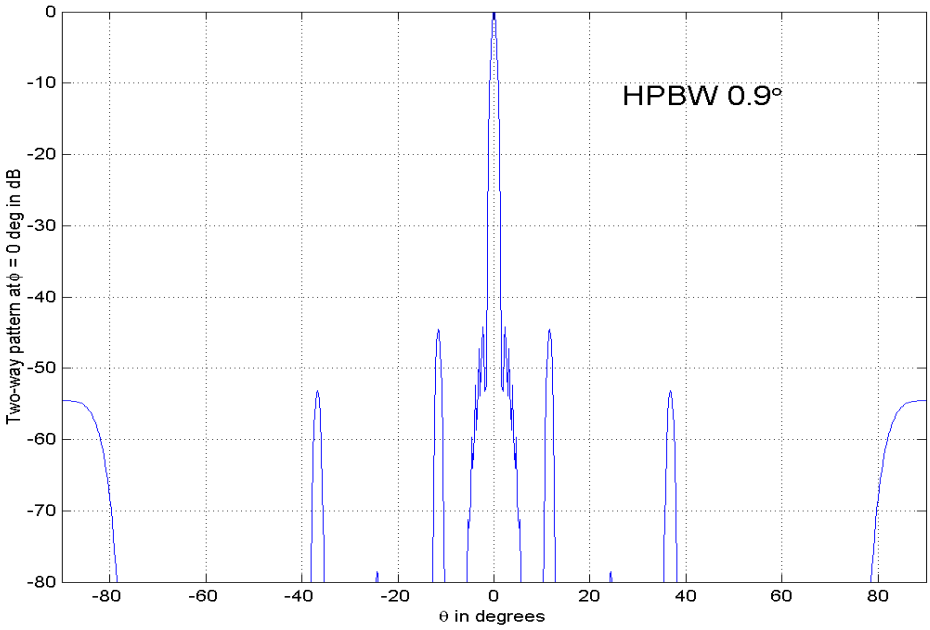

Figure 19. Two-way H-plane broadside pattern of MFAR DSA

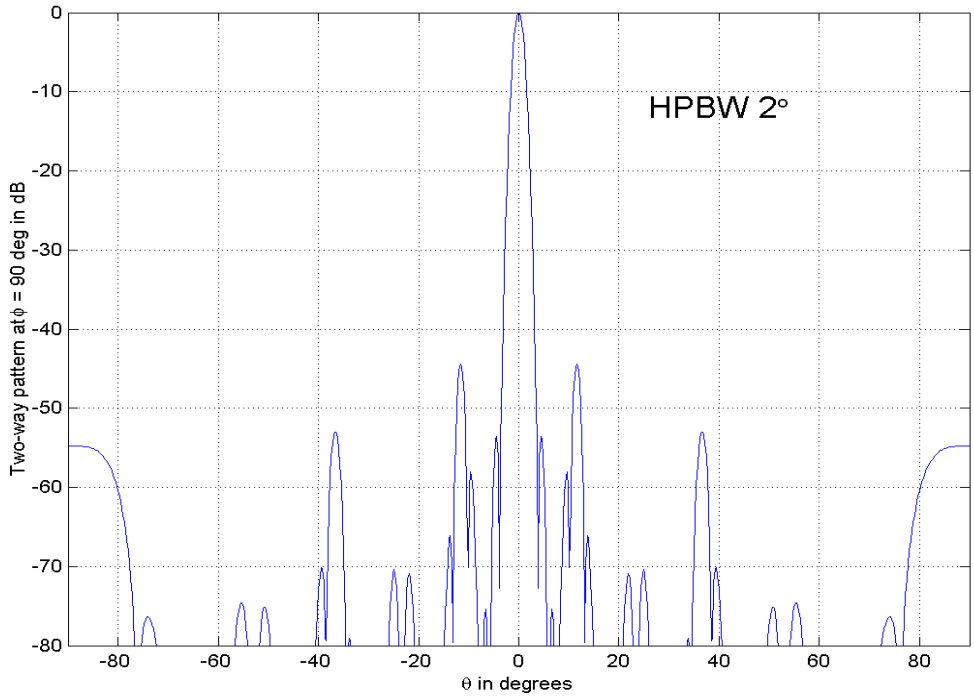

Figure 20. Two-way E-plane broadside pattern of MFAR DSA

Figures 21 and 22 show the receive patterns when the beam is scanned to $\theta_s = 10°$ and $60°$ respectively. The nulling effect of subarray factor on the configuration factor is unchanged with scan. The transmit pattern broadens from scanning at the same rate as the receive pattern broadens. Figures 23 and 24 show the two-way pattern scanning to $\theta_s = 10°$ and $60°$, Figure 25 shows the two-way pattern of multiple beams scanned at increments of $\Delta\theta = 5°$.

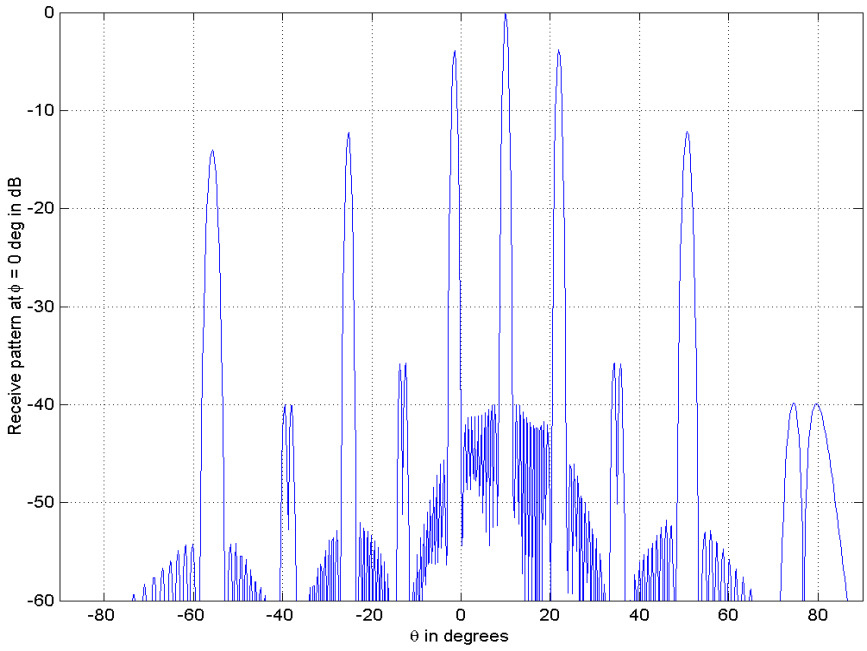

Figure 21. Receive pattern of 16 subarrays when scanned to 10° from H-plane broadside

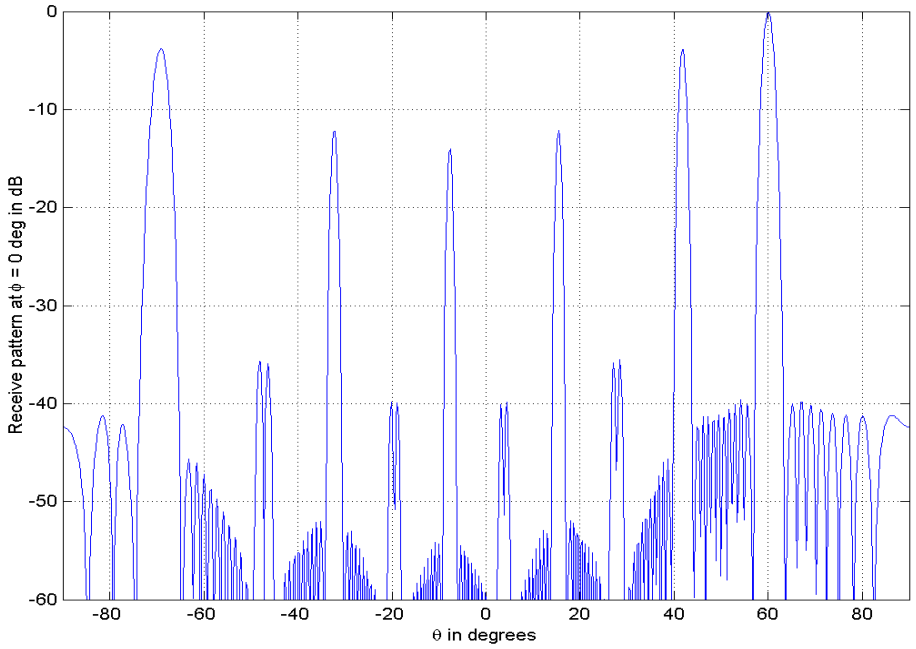

Figure 22. Receive pattern of 16 subarrays scanned to 60° from H-plane broadside

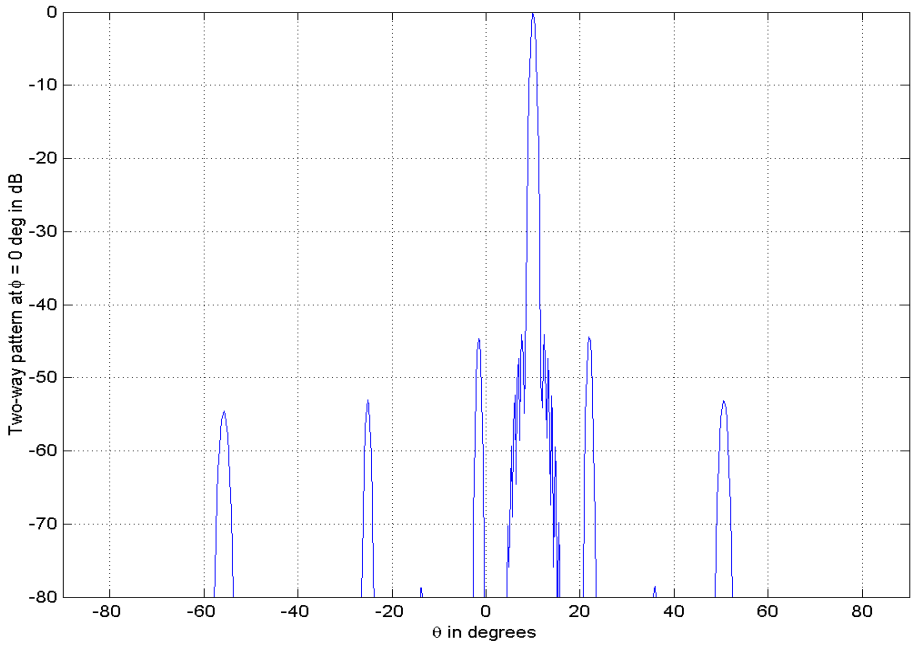

Figure 23. Two-way pattern scanned to 10° from broadside

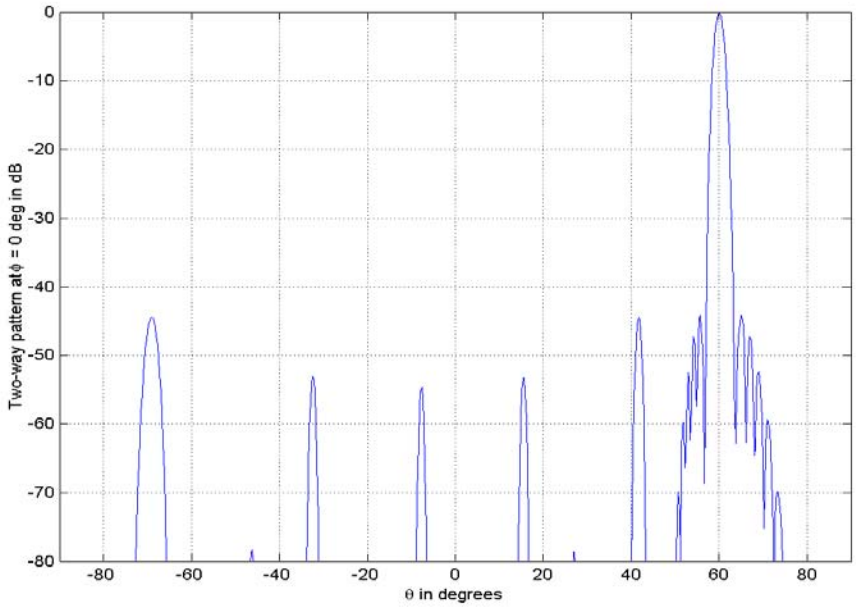

Figure 24. Two-way pattern scanned to $60°$ from broadside

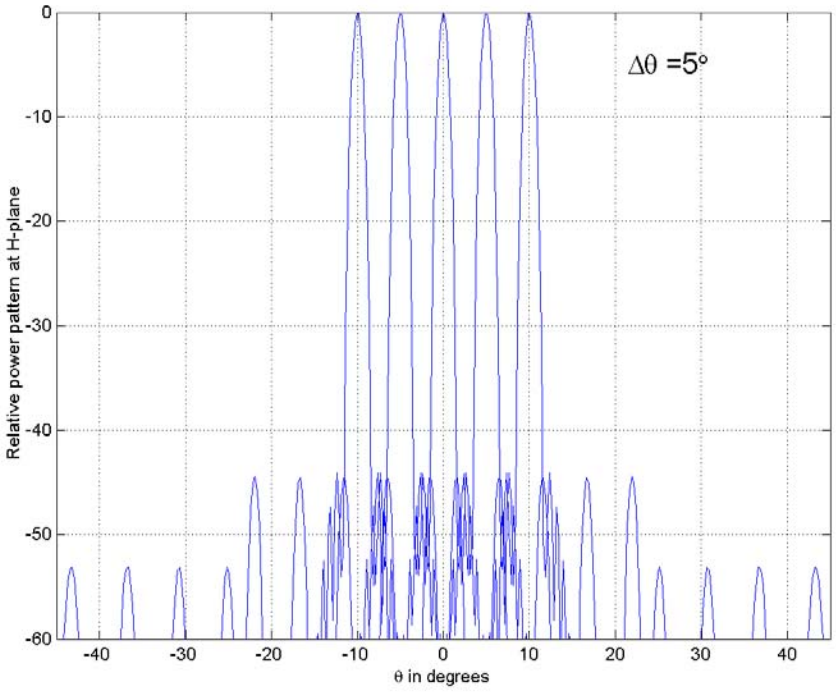

Figure 25. Multiple beams scanning with θ_s increments $5°$

3. Shipboard HF and VHF Distributed Subarray Antennas

The other possible application of DSA onboard a ship is at the lower frequencies. Lower frequencies have better performance for long-range surveillance, especially on targets with small RCS because HF and VHF are in the resonance region for the targets of interest (e.g., cruise missiles). However, a major problem is how to increase the resolution from the limited small areas on a ship. By processing signals coherently from several separate subarrays, the half power beamwidth can approach λ / L, where L can be the total length of the ship.

Figure 26 is the side view of an AEGIS cruiser, with some possible areas, marked as 1 to 4, on which subarrays could be placed. The locations are detailed in Figure 27. For simplicity, it is assumed that these four subarrays are all flat and rectangular in shape. The number of elements is 12, 6, 7 and 13, respectively (along the x-axis). The physical limitations in this case are significant, and the number of elements is so few that a straight forward combination of the four areas does not yield any reasonable performance at VHF. The placement of elements in each subarray needs to be optimized by the Minimax method in Section A to decrease the level of the grating lobes.

By fixing the position of the edge elements in each subarray, the Minimax algorithm finds the optimized positions for minimum peak SLL in the array factor. Since subarrays 1 and 2 and subarrays 3 and 4 overlap along the x-axis, and the maximum possible distance is between subarrays 1 and 4, there are only two possible combinations of subarrays to produce a low SLL pattern for the requirement of high resolution. The first combination is to process all four subarrays coherently as a monostatic radar. A plot of the array factor and the equivalent two-way pattern is shown in the Figures 28 and 29 for combination 1.

A second possible combination is to use subarrays 1 through 3 as the receive pattern, and then synthesize a transmit pattern for subarray 4 by the equiripple method discussed in the Section A. A plot of the receive pattern (3 subarrays) is given in Figure 30, and the two-way pattern in Figure 31. The optimized element positions for the 2 combinations are shown in the Tables 1 and 2.

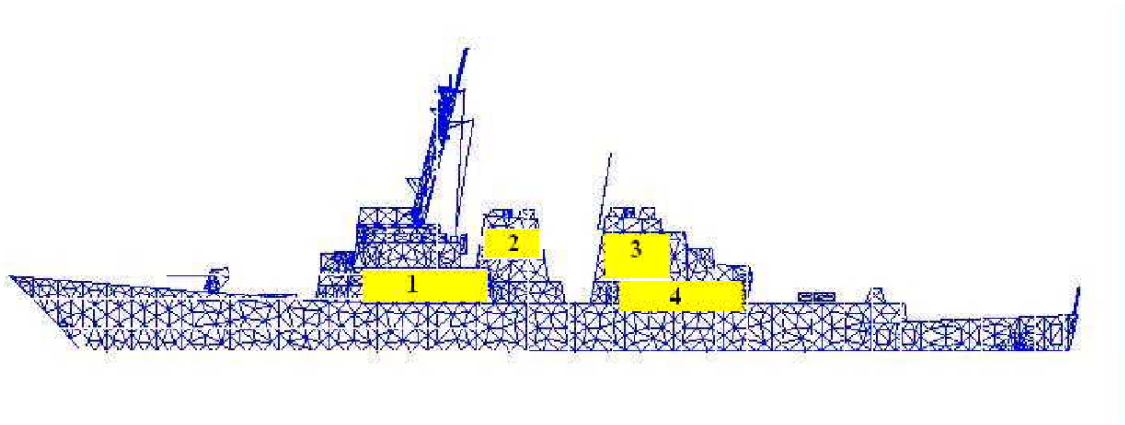

Figure 26. Side view of the Aegis cruiser

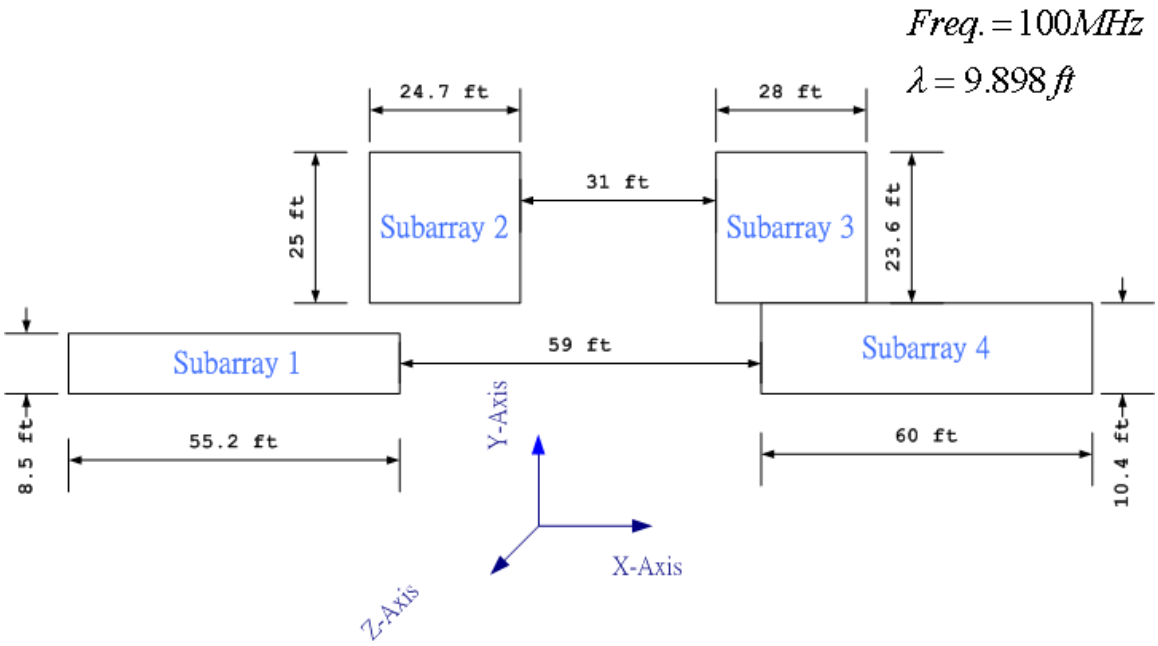

Figure 27. Possible locations of VHF subarrays on the Aegis cruiser

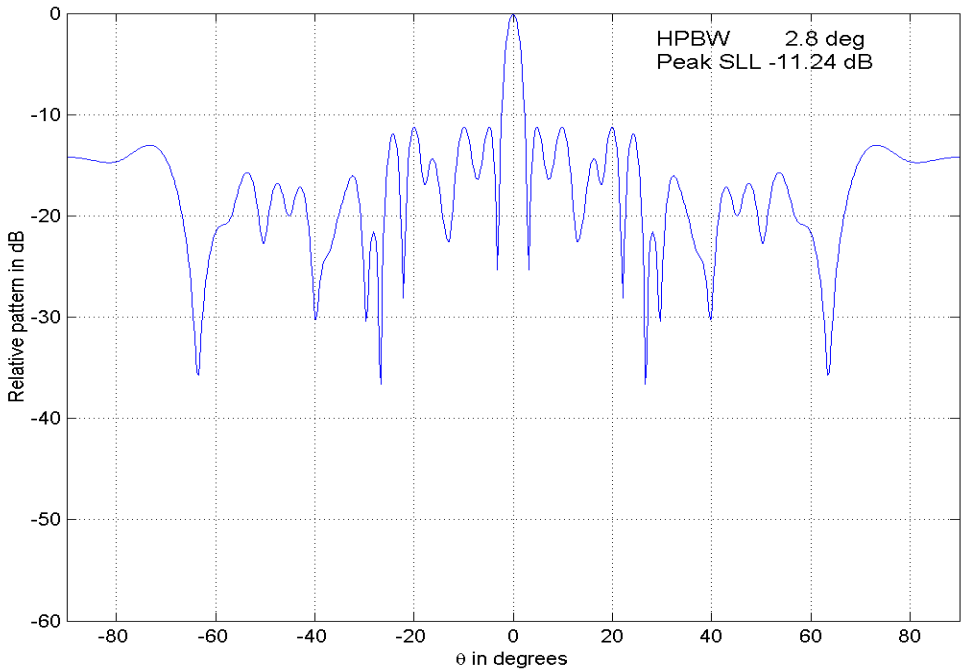

Figure 28. Combination 1: Pattern of the 4 subarrays processed coherently to form a single array used for both transmit and receive.

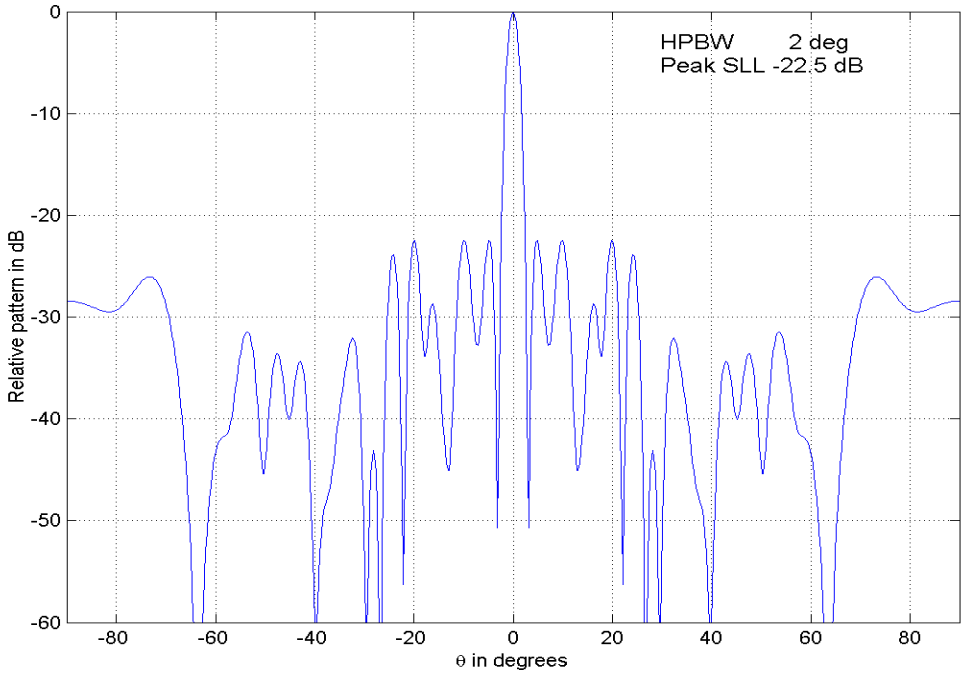

Figure 29. Combination 1: Equivalent 2-way pattern of the monostatic array.

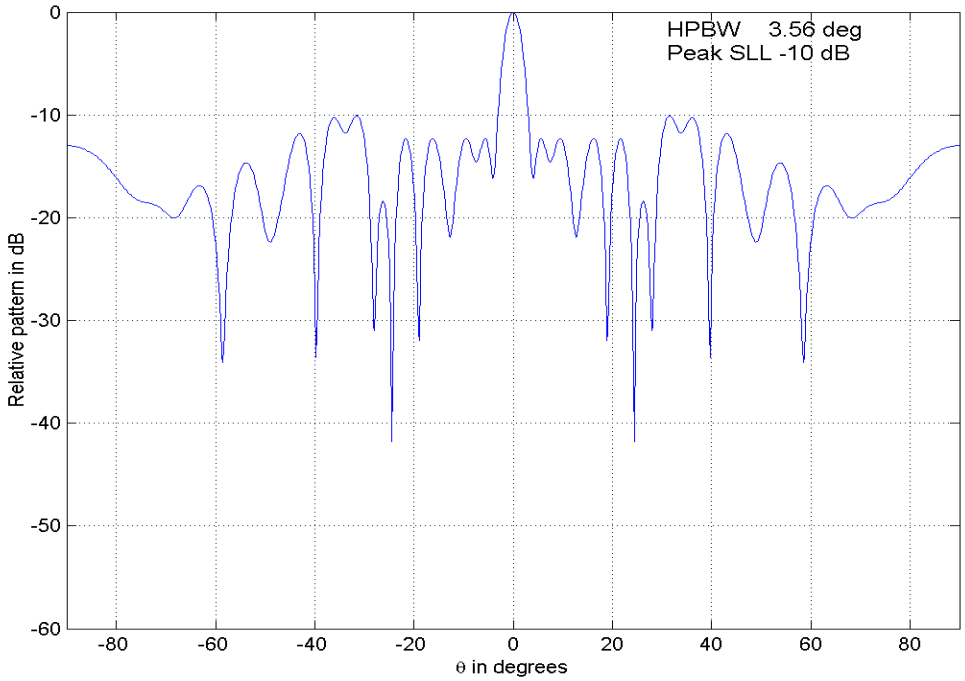

Figure 30. Combination 2: Receive pattern using 3 subarrays

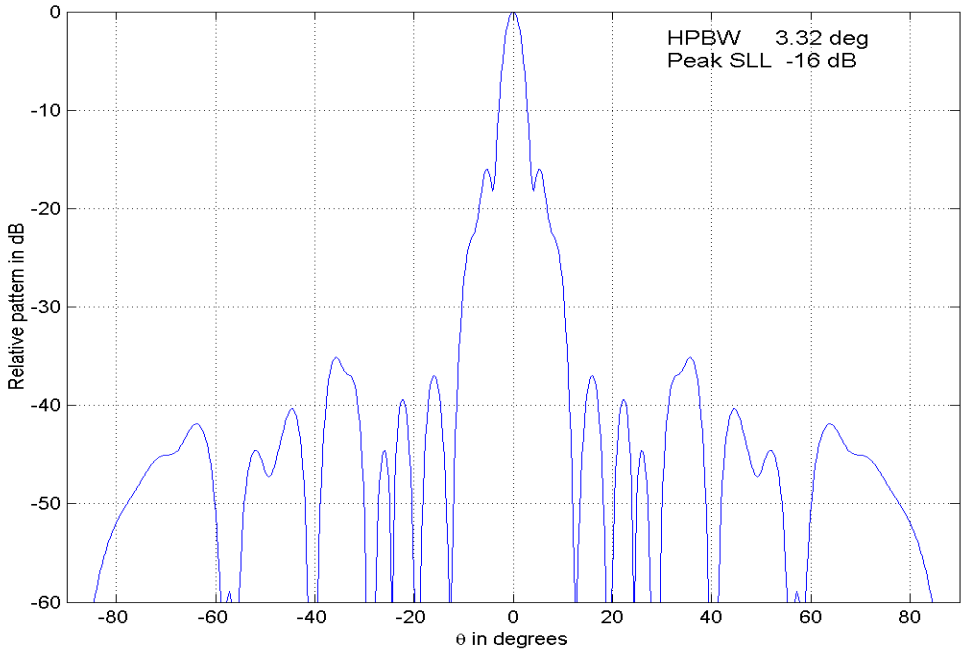

Figure 31. Combination 2: Two-way pattern (3 receive subarrays and 1 transmit subarray).

Element position in λ	Subarray 1	Subarray 2	Subarray 3	Subarray 4
x_1	0	5.1090	10.7439	11.5530
x_2	0.0073	6.0490	10.7659	11.5588
x_3	0.5146	6.5390	11.2379	12.0647
x_4	2.0219	7.0290	11.7099	12.5705
x_5	2.5292	7.5190	12.1819	13.9289
x_6	3.0365	7.6070	12.6539	14.5822
x_7	3.5438		13.5760	14.6629
x_8	4.0511			14.9961
x_9	4.5071			15.0996
x_{10}	5.0657			16.6055
x_{11}	5.5730			17.1113
x_{12}	5.5800			17.6171
x_{13}				17.6230

Table 1. Optimized locations of elements in the 4 subarrays for combination 1.

Element position in λ	Subarray 1	Subarray 2	Subarray 3	Subarray 4
x_1	0	5.1090	10.7439	0
x_2	0.0073	6.0490	10.7659	0.5
x_3	0.5146	6.5390	11.2379	1
x_4	2.0219	7.0290	11.7099	1.5
x_5	2.0464	7.5190	12.1819	2
x_6	2.8683	7.6070	13.5539	2.5
x_7	3.5438		13.5760	3
x_8	3.6610			3.5
x_9	3.6706			4
x_{10}	4.4881			4.5
x_{11}	5.5730			5
x_{12}	5.5800			5.5
x_{13}				6

Table 2. Optimized locations of elements in the 4 subarrays in combination 2.

Combination 1, which uses all 4 subarrays, gives better performance for both the peak SLL (-22.5 dB) and the beamwidth (2°) for the round trip pattern as shown on Figure 29. However, Combination 2 has a much lower average SLL than Combination 1, and the individual use of subarray 4 gives more flexibility on the design of two-way pattern.

These two distributed VHF subarray designs demonstrate the possibility of maximizing the resolution given the space limitation onboard the ship. This simple algorithm of pattern design does not show the full potential of unequal sized or nonuniform spacing subarrays. Other suitable algorithms, like the Genetic Algorithm (GA), may provide better solutions for these types of problem [Ref. 16].

4. Calculation of Antenna Parameters on MFAR DSA Design

Since the DSA has a large spacing between subarrays, the simple formulas for antenna parameters need modification from those for conventional filled arrays. The following paragraph will show analytical and simulated results of these important parameters of the MFAR DSA. The pattern parameters will be examined for the antenna design described in Section 2.

(a) Two-way beamwidth between first nulls

Since the result of the two-way pattern is the product of transmit and receive patterns, by the principle of pattern multiplication, the two-way BWFN is a function of both patterns. The BWFN of the receive pattern, from Equation (2), is mainly dependent on the subarray configuration factor, which varies as $\sin(N\psi/2)$ in the uniform DSA design. The BWFN of transmit pattern, however, is determined by the Chebyshev coefficients, which are controlled by the sidelobe level, number of elements, interelement spacing and the frequency. The transmit BWFN is not easy to calculate analytically, especially for the two-way pattern. Theoretically, since the beamwidth of the receive pattern is sharper than that of transmit pattern, the shape of the mainlobe at broadside is determined mainly by the receive pattern. The BWFN of the receive pattern is approximately $3.2°$ at the H-plane broadside measured from the pattern plot on Figure 17.

(b) Two-way half power beamwidth

Since the two-way mainlobe is determined mainly by the receive pattern, the HPBW of the two-way pattern can be approximately determined by the receive pattern also, which is

$$\left|AF_{norm}(u)\right|^2 = \left|\frac{\sin(\frac{M\xi}{2})}{M\sin(\frac{\xi}{2})}\frac{\sin(\frac{N\psi}{2})}{N\sin(\frac{\psi}{2})}\right|^2 = 0.5\,. \qquad (14)$$

It is assumed uniform weighted on both subarrays and elements. Since $N\psi \gg M\xi$, and the phase term of subarray configuration is changing much faster than the phase of subarray factor, the HPBW is determined mainly by the subarray configuration factor.

λ = *wavelength; D = aperture wideth*

Type of distribution, $\lvert z\rvert < 1$	Relative gain	Half-power beamwidth, deg	Intensity of first sidelobe, dB below maximum intensity
Uniform; $A(z) = 1$	1	$51\lambda/D$	13.2
Cosine; $A(z) = \cos^n(\pi z/2)$:			
$n = 0$	1	$51\lambda/D$	13.2
$n = 1$	0.810	$69\lambda/D$	23
$n = 2$	0.667	$83\lambda/D$	32
$n = 3$	0.575	$95\lambda/D$	40
$n = 4$	0.515	$111\lambda/D$	48
Parabolic; $A(z) = 1 - (1 - \Delta)z^2$:			
$\Delta = 1.0$	1	$51\lambda/D$	13.2
$\Delta = 0.8$	0.994	$53\lambda/D$	15.8
$\Delta = 0.5$	0.970	$56\lambda/D$	17.1
$\Delta = 0$	0.833	$66\lambda/D$	20.6
Triangular; $A(z) = 1 - \lvert z\rvert$	0.75	$73\lambda/D$	26.4
Circular; $A(z) = \sqrt{1 - z^2}$	0.865	$58.5\lambda/D$	17.6
Cosine-squared plus pedestal;			
$0.33 + 0.66\cos^2(\pi z/2)$	0.88	$63\lambda/D$	25.7
$0.08 + 0.92\cos^2(\pi z/2)$, Hamming	0.74	$76.5\lambda/D$	42.8

Table 3. Pattern characteristics produced by various aperture distributions [from Ref. 10].

For a Hamming window distribution, the HPBW is approximately $76.5\lambda / L$ from Table 3. For $N = 16,\ D = 5\lambda,\ L = 15 \times 5 + 2 = 77\lambda$, by the parameters of MFAR DSA design in Section 2, the broadside HPBW is approximately 1°. This value is a little larger than the measured value of $0.9°$ from the two-way pattern on Figure 19 because of the multiplication between the transmit and receive pattern. Compared to a fully populated uniform array $(\lambda/2)$, it is necessary to have 115 linear uniform weighted elements to have the same resolution. It is achieved using 80 linear elements with the DSA approach.

(c) Aperture efficiency and directivity

Since the receive DSAs are Hamming weighted at the subarray level, the taper efficiency (receive aperture efficiency) is 0.47 using Equation (3). The efficiency of the transmit pattern by the same equation is 0.6. However the directivity cannot be calculated by the equation $D = 4\pi\eta A\cos\theta_s / \lambda^2$, because grating lobes exist. The area A is the area occupied by array elements.

By definition, the directivity is the ratio of the radiation intensity to the average radiation intensity, or [Ref. 7]

$$D(\theta,\phi) = \frac{4\pi}{\Omega_A}, \tag{15}$$

where $\Omega_A = \int_0^{2\pi}\int_0^{\pi} \left|\vec{E}_{norm}\right|^2 \sin\theta d\theta d\phi$ is the beam solid angle, and $\vec{E}_{norm}$ is the normalized electric field intensity. Neglecting the element factor, $\vec{E}_{norm}$ is the normalized total array factor. By numerical integration of the normalized array factor in spherical coordinates, the directivity calculated from Equation (15) is about 40 dB for a uniform weighted DSA, which is almost the same value calculated from the same number of elements (80×40) in contiguous spacing $(\lambda/2)$. Considering the tapering, the directivity of the Hamming weighted DSA is about 36.7 dB, the directivity of the transmit arrays $(35 \times 35$ elements) is about 32.7 dB, and the equivalent one-way antenna gain $G = \sqrt{G_t G_r} \simeq 34.7$ dB. This result shows that the gain of DSA antenna depends directly on the number of elements and taper efficiency.

Table 4 summarizes the antenna parameters for a DSA (receive subarray) design ($N=16$, $M=5$, $D_x=5\lambda$, $D_y=5\lambda$, $d_x=0.5\lambda$, $d_y=0.5\lambda$). An effective area of $(0.5\lambda)^2$ is assumed for each element. The results show that the approximate formula for directivity ($D=4\pi\eta A\cos\theta_s/\lambda^2$) is not correct in the DSA application, unless the occupied area is used.

	Approximate formula (uniform weight)	**Actual computed (uniform weight)**	**Hamming weight on subarrays**
BWFN	1.43°	1.43°	3.25°
HPBW	0.66°	0.64°	0.94°
DIRECTIVITY	45.5 dB (total area) 40 dB (active area)	40 dB	36.7 dB
MAX SLL	-13.2 dB	-13.2 dB (SLL) -3.8 dB (grating)	-39 dB (SLL) -3.8 dB (grating)

Table 4. Summary of antenna pattern parameters for MFAR DSA.

C. SUMMARY

This chapter has presented the basic theory and methods of subarraying. There are two approaches to reducing grating lobes due to the large spacing between subarrays in a periodic DSA. The first approach is placing the nulls of one factor (AF_s and AF_{Tx}) in the direction of grating lobes of the other factor (AF_c). The second approach is to use irregular spaced subarrays to reduce the peak grating lobes by redistributing the energy into sidelobe regions.

Two possible applications of DSA onboard a ship have been introduced in this chapter. MFAR DSA can be used at higher frequencies (X or C band) to reduce the cost and weight of modern radar. At lower frequencies (HF or VHF band), the application of DSA can increase the resolution obtained from utilizing the limited small areas on a ship. This is important for detecting and tracking targets with small RCS like cruise missiles.

The calculation of antenna parameters of the DSA design shows the tradeoff in performance on the directivity and beamwidth. The directivity depends on the number of elements and tapering only; the beamwidth decreases as the subarray spacing increases.

THIS PAGE INTENTIONALLY LEFT BLANK

IV. CONCLUSION

A. SUMMARY

The concept of distributed subarray antennas has been proposed for both the MFAR and VHF applications. By combining distributed subarrays on the available areas of a constrained platform, the MFAR or VHF DSA can achieve the maximum resolution (aside from synthetic aperture approaches) and potential reductions in cost and complexity. The two-way pattern design of a DSA effectively suppressed the undesired grating lobes by the design of separate transmit and receive patterns. From the pattern multiplication principle, the grating lobes in the subarray configuration pattern (AF_c) have been suppressed by the design of subarray pattern (AF_s) and transmit pattern (AF_{Tx}).

The design examples of shipboard MFAR have shown that the HPBW decrease (increased resolution) can be achieved by spreading a fewer number of elements over a longer baseline and then suppressing the grating lobes with other pattern factors. The nulling effect of the subarray factor does not change as the beam scans away from broadside. The limitations and advantages of DSA have been mentioned previously throughout the thesis, and are summarized here.

1. Advantages of the MFAR DSA

a. Support of Wideband ADBF

The collection of elements is steered in phase at the element level, and a beamforming network combines the element into subarrays. The subarrays are then steered via photonic time delay devices. This provides the necessary wideband beam steering and ADBF capabilities at a reasonable cost.

b. Support of Multi-functionality

Since each subarray is physically separated, a separate function can be assigned each subarray more directly. The design of subarrays can be more adaptive to the main function from the design stage, which decreases the effects of compromises on performance.

c. Low Complexity of Manufacturing and Computing with Less Control Elements

Although some compromises between performance and periodic spacing have been made, regularity makes the implementation of subarrays more realistic and practical for the requirements of modern radar. However, irregular placement of elements is not a huge disadvantage. Randomly thinned arrays have been used for radars in the past [Ref. 16].

d.Achieving High Resolution with Less Space Limitation

The required angular accuracy and range resolution can be achieved with little limitation on platform space. Little perturbations in subarray locations do not have much effect on the array pattern. The arrangement and dimensions of the subarrays can be adjusted to the shape of platform.

e. Possibility of Multi Band Shared Apertures

Since the spacing between the subarrays is large, it is possible to insert other low frequency elements to share the same aperture space. For example, if the subarrays structure is designed for X-band frequencies, then an L-band array element can be inserted between subarrays with half wavelength spacing. Figure 32 shows a possible scheme for a X and L band array.

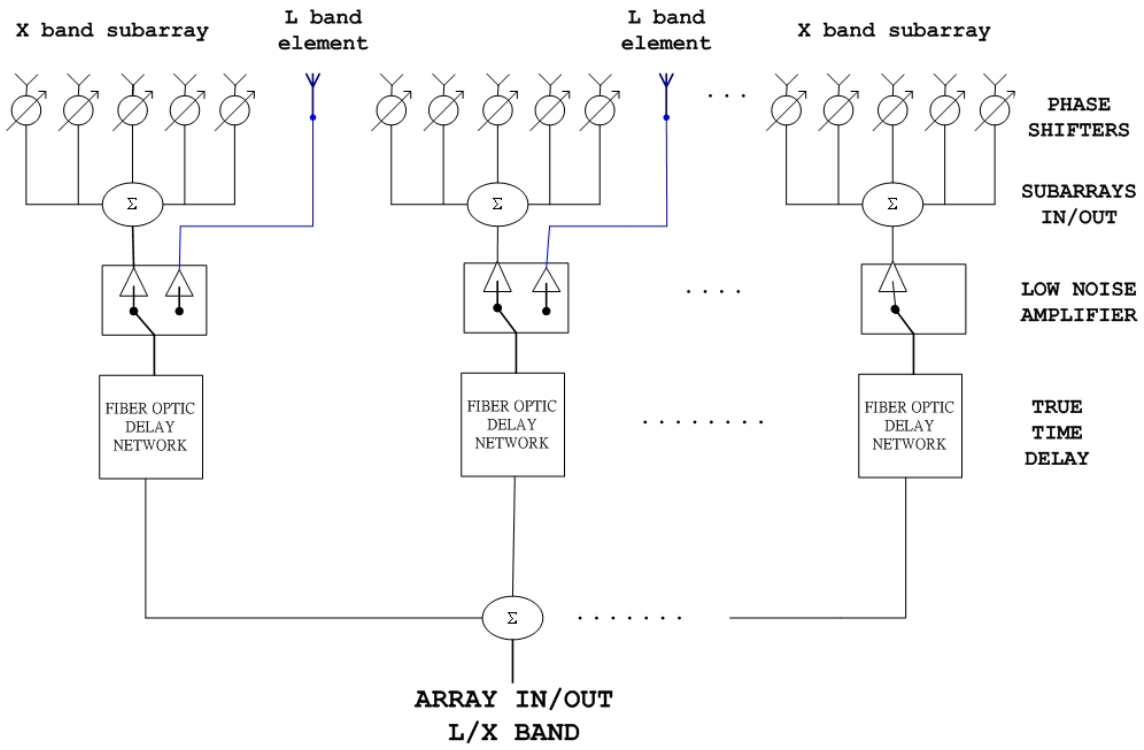

Figure 32. Possible beam control scheme of a dual-band DSA [after Ref. 17]

2. Limitations of the MFAR DSA Design

a. Less Efficiency on Surveillance Due to the Narrow Beamwidth of Transmit Pattern

If the beamwidth of the transmit pattern is tied to the synthesis of the two-way pattern, the resulting beam may not provide a large enough field of view for searching. This disadvantage, however, can be corrected by dividing the transmit pattern into searching and tracking modes. In the search mode, the center transmit/receive module operates alone like any other element-based phased array. In the tracking mode, the center transmit module is a high contrast pencil beam, and the resultant two-way pattern is the multiplication of transmit and receive pattern synthesized for the DSA. A dual-band shared aperture is another possible approach for separating the track and surveillance into different combinations; for examples, long-range surveillance (L band), mid-range surveillance (X band) and tracking (X band DSA).

b. Lower Beam Efficiency Due to the Grating Lobes

From the calculations in Chapter III, the antenna directivity depends only on the area occupied by elements. There is a reduction in beam efficiency resulting from the grating lobes, and any sidelobe taper will lower the efficiency further (typically about 3 dB). However, this can be improved at the expense of more subarrays or closer spacing between them

c. Fewer Degrees of Freedom on Pattern Synthesis

Since the number of individual control elements is decreased by the subarray design, the degrees of freedom (DOF) in terms of ADBF capability is decreased substantially. The limitations resulting from the synthesis of transmit and receive patterns also restrict the implementation of DSA in the environment of high clutter because of lower sensitivity and less capability for nulling interferences.

d. More Complexity of Task Scheduling

Having a multifunction radar complicates the task scheduling of a single antenna. The two-way pattern approach introduces more constraints on the scheduling tasks. The time budget i.e., the allocation of radar time to different tasks is dependent on the radar antenna parameters. Since the main tasks of MFAR are search, track and other auxiliary functions, the strategy of how to execute of all tasks in the best possible way is very complicated.

B. POSSIBLE FURTHER RESEARCH TOPICS

There are two primary directions of research on suppressing the grating lobes in the pattern of widely spaced subarrays, as discussed below.

1. Filtering Approach

There are many filtering techniques already developed in the area of digital signal processing. If the main objective is to suppress the grating lobes from self-interference, the adaptive notch filter (ANF) or space-time domain adaptive processing (STAP) might be the possible research area for the implementation of DSA.

Adaptive notch filters are widely used in many signal-processing applications to extract and trace the narrow-band noise. The basic principle is to produce the adaptable frequency response in both the time and space domain: zero at the specified spatial angle, one otherwise. Figure 33 shows the example of frequency response on nulling the angles $\pm 15°$ and $\pm 37°$, everywhere else unchanged. The depth and width of nulls should be adjusted according the grating conditions. But this must be implemented in both the space and time domain, which introduces the applications of the STAP algorithm [Ref. 18]. For a DSA the notches would be placed at grating lobe locations.

STAP processes signals in the spatial and time domains. The time domain includes both slow-time (pulse repetition interval) and fast-time (range cell). Therefore, the utilization of phase and amplitude weighting as a means to achieve a desired steering or nulling direction must consider the spatial, slow-time and fast-time factors.

2. Digital Arrays

Unlike an analog beamforming network, digital beamforming arrays digitize received signals at the element level, then process these signals in a digital processor to form the desired beam and frequency response (in this case, nulling in the grating direction). By doing so, the total information available at the aperture has been properly preserved and can be manipulated indefinitely without introducing further error (other than computer roundoff error).

Adaptive digital beamforming at the element level can reject interference and at the same time steer a main lobe in the direction of a desired signal. Therefore, any number of beams can be formed or the signal can be rejected according to a selected algorithm.

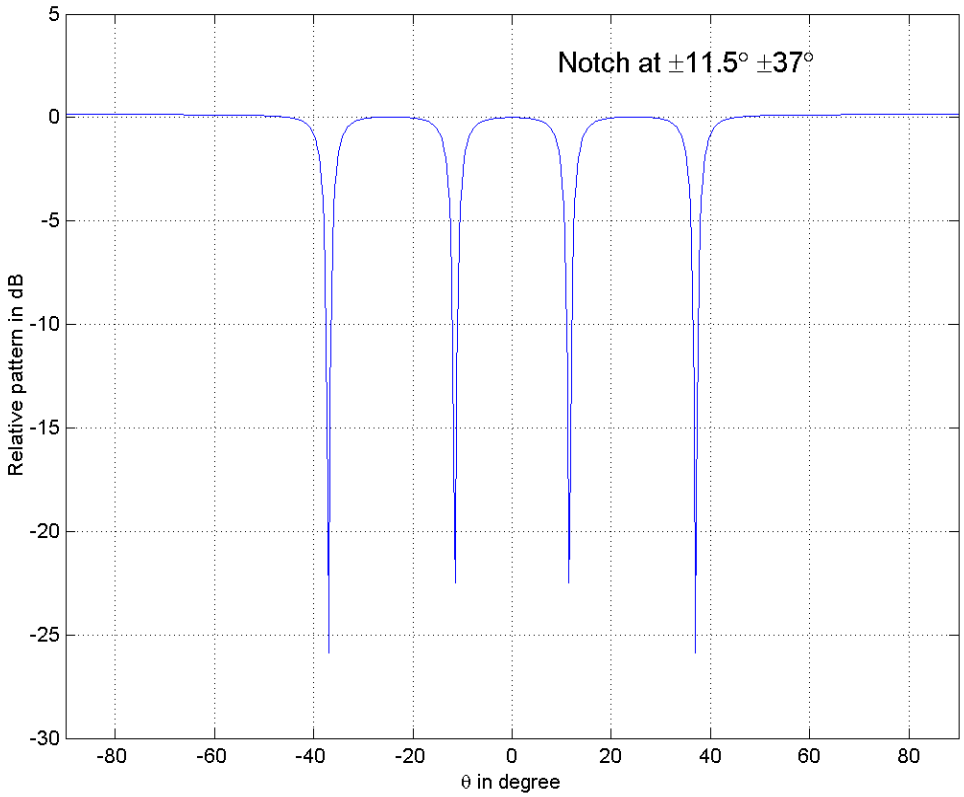

Figure 33. Adaptive nulling at the angle ±15°, ±37° by ANF.

APPENDIX A: GLOSSARY OF TERMINOLOGY

MFAR	Multi-function Array Radar
ADBF	Adaptive Digital Beamforming
LPI	Low Probability of Intercept
MFSAR	Multifunction Subarray Radar
dB	Decibels
mrad	milli radian (10^{-3} radian)
MHz	Megahertz (10^{6} cycles/second)
GHz	Gigahertz (10^{9} cycles/second)
MESAR	Multifunction Electronically Scanned Adaptive Radar
TWS	Track-While-Scan
AF	Array Factor
AF_s	Subarray Factor
AF_c	Subarray Configuration Factor
AF_{Tx}	Transmit Array Factor
AF_{Rx}	Receive Array Factor
EF	Element Factor
BWFN	Beamwidth Between First Nulls
HPBW	Half Power Beamwidth
λ	Lambda — wavelength
SNR	Signal-to-Noise Ratio
RCS	Radar Cross Section

SLL	Sidelobe Level
DSA	Distributed Subarray Antenna
FIR	Finite Impulse Response
WLS	Weighted Least Squares algorithm
Tx	Transmitter
Rx	Receiver
HF	High Frequency (3 ~ 30 MHz)
VHF	Very High Frequency (30 ~ 300 MHz)
UHF	Ultra High Frequency (300 ~ 3000 MHz)
DOF	Degree Of Freedom
ANF	Adaptive Notch Filter
STAP	Space Time Adaptive Processing

APPENDIX B: MATLAB CODE LISTING

The major MATLAB Code listing for the pattern plot as the following.

```
%%%%%%%%%%%%%%%%%%%%%%%%%%%%%%%%%%%%%%%%%%%%%%%%%%
% DSA.m
% Pattern calculation and plot for Figure 8,13,14,18-25
% Quasi-monostatic subarrays AF
% XMTR AF has 35x35 Remez-weighted elements spacing 0.5 wavelength
% RCVR is 16x8 subarrays with 5x5 elements in each subarray
% Each subarray spacing 5 wavelengths in x&y axis with Hamming weights
% Display the aperture efficiency also
% resolution of plot is quarter degree

clear all;
llx=0:5:75;  % 16 Subarray spaced (Lambda) in x-axis
lly=0:5:35;  % 8 Subarray spaced in y-axis
dx=0.5; Mx=5; % element spacing and number in subarray along x-axis
dy=0.5; My=5; % element spacing and number in subarray along y-axis

% Scan angle input
% Figure 21-25 need to change angle accordingly
thets=0;
phis=0;
us=sin(thets*pi/180)*cos(phis*pi/180);
vs=sin(thets*pi/180)*sin(phis*pi/180);

thet=linspace(-90,90,720);  % x,y direction cosine
theta=thet.';
phi=linspace(0,180,720);
u=sin(theta*pi/180)*cos(phi*pi/180);
v=sin(theta*pi/180)*sin(phi*pi/180);
U=u-us;
V=v-vs;
% Subarray configuration AF
% Weighting Function by Hamming window
```

```
wx=zeros(1,length(llx));  % weights in x-axis
for n=1:length(llx)
   xn=(n-1)/(length(llx)-1)*2-1;
   wx(n)=0.92*abs(cos(xn*pi/2))^2+0.08;
end

wy=zeros(1,length(lly));  % weights in y-axis
for n=1:length(lly)
   yn=(n-1)/(length(lly)-1)*2-1;
   wy(n)=0.92*abs(cos(yn*pi/2))^2+0.08;
end

CAFx=zeros(720);
for lx=1:length(llx)
   psilx=2*pi*llx(lx)*U;
   CAFx=CAFx+wx(lx)*exp(j*psilx);
end

CAFy=zeros(720);
for ly=1:length(lly)
   psily=2*pi*lly(ly)*V;
   CAFy=CAFy+wy(ly)*exp(j*psily);
end
CAF=CAFx.*CAFy/sum(wx)/sum(wy);

% Single subarray AF
SAFx=zeros(720);
for sx=1:Mx
   psix=2*pi*dx*U;
   SAFx=SAFx+exp(j*(sx-1)*psix);
end
SAFy=zeros(720);
for sy=1:My
   psiy=2*pi*dy*V;
   SAFy=SAFy+exp(j*(sy-1)*psiy);
end
SAF=SAFx.*SAFy/Mx/My;
```

```
% XTMR array design to pass mainlobe, others with 45 db attenuation
% First calculation the equal ripple coefficients
% use for obtaining 9 deg mainlobes, every other angle response -40 db
px=35;              % Element numbers in x-axis
fs=90;              % Array factor half space
rp=1;               % Passband ripple in db
rs=-50;             % Stopband desired attenuation in db
fc=[0 4.5];         % Cutoff spatial freq
a=[1 0];            % Desired amplitude
dev=[(10^(rp/20)-1)/(10^(rp/20)+1) 10^(rs/20)]; % dB to numerical
[nx,f0x,a0x,Wx]=remezord(fc,a,dev,fs);
bx=remez(px-1,f0x,a0x,Wx); % Using fixed number elements
bx=abs(bx(1:length(bx)));  % Elements weighting
Bx=bx/max(bx);             % Normalized weights

py=35;              % element # in y-axis
fs=90;              % Array factor half space
rp=1;               % Passband ripple in db
rs=-50;             % Stopband attenuation in db
fC=[0 4.5];         % Cutoff spatial freq(angle)
a=[1 0];            % Desired amplitude
dev=[(10^(rp/20)-1)/(10^(rp/20)+1) 10^(rs/20)];
[ny,f0y,a0y,Wy]=remezord(fC,a,dev,fs);
by=remez(py-1,f0y,a0y,Wy); % Using fixed number elements
by=abs(by(1:length(by)));  % elements weighting
By=by/max(by);                % Normalized weights

% Array factor in square XTMR
XAFx=zeros(720);
for Xx=1:length(Bx)
   psiXx=2*pi*dx*U;
   XAFx=XAFx+Bx(Xx)*exp(j*(Xx-1)*psiXx);
end
XAFy=zeros(720);
for Xy=1:length(By)
   psiXy=2*pi*dy*V;
```

```
   XAFy=XAFy+By(Xy)*exp(j*(Xy-1)*psiXy);
end
% calculate RCVR aperture efficiency
    Rs1=0; Rs2=0;
    for i1=1:length(llx)
        for i2=1:length(lly)
            Rs1=Rs1+abs(wx(i1)*wy(i2)); Rs2=Rs2+abs(wx(i1)*wy(i2))^2;
        end
     end
 eta=Rs1^2/length(llx)/length(lly)/Rs2;
% calculate XTMR aperture efficiency
    Xs1=0; Xs2=0;
    for i1=1:length(Bx)
        for i2=1:length(By)
            Xs1=Xs1+abs(Bx(i1)*By(i2)); Xs2=Xs2+abs(Bx(i1)*By(i2))^2;
        end
    end
 ETA=Xs1^2/length(Bx)/length(By)/Xs2;
  disp(['RCVR aperture efficiency: ',num2str(eta)])
  disp(['XTMR aperture efficiency: ',num2str(ETA)])

% XTMR AF
XAF=(XAFx.*XAFy)/sum(Bx)/sum(By);
dbXAF=20*log10(abs(XAF));
% RCVR AF
RAF=SAF.*CAF;
dbRAF=20*log10(abs(RAF));
% Two-way pattern
BAF=XAF.*RAF;
dbBAF=20*log10(abs(BAF));  % 2-way pattern in dB
dbSAF=20*log10(abs(SAF));  % Subarray pattern in dB
dbCAF=20*log10(abs(CAF));  % Subarray configuration pattern in dB

figure(1)  % Figure 8
subplot(3,1,1), plot(theta(1:720), dbRAF((1:720),phis+1)),axis([-90 90 -60 0]),
grid on, title(' Receive pattern of 16 subarrays spacing 5\lambda')
subplot(3,1,2), plot(theta(1:720), dbSAF((1:720),phis+1)),axis([-90 90 -60 0]),
```

```
grid on, title(' Pattern of single subarray which is composed by 5 elements')
ylabel('Relative pattern at \phi=0\circ in dB')
subplot(3,1,3), plot(theta(1:720), dbCAF((1:720),phis+1)),axis([-90 90 -60 0]),
grid on, title(' Pattern of 16 subarray configuration')
xlabel('\theta in degree')

figure(2)
subplot(3,1,1), plot(theta(1:720), dbBAF((1:720),phis+1)),axis([-90 90 -100 0]),
grid on, title(' Two Way pattern of 16 subarrays spacing 5\lambda')
subplot(3,1,2), plot(theta(1:720), dbRAF((1:720),phis+1)),axis([-90 90 -100 0]),
grid on, title(' Receive pattern of 16 subarrays spacing 5\lambda')
ylabel('Relative pattern at \phi=0\circ in dB')
subplot(3,1,3), plot(theta(1:720), dbXAF((1:720),phis+1)),axis([-90 90 -100 0]),
grid on, title(' Transmit pattern of 35 elements')
xlabel('\theta in degree')

figure(3) % Figure 18
% Receive pattern of 16 subarrays spaced 5 wavelength
plot(theta(1:720), dbRAF(1:720,phis+1)),axis([-90 90 -60 0]),
grid on,
ylabel('Receive pattern at \phi = 0 deg in dB')
xlabel('\theta in degrees')

figure(4) % Figure 13
% Transmit pattern of 35 elements
plot(theta(1:720), dbXAF(1:720,phis+1)),axis([-90 90 -80 0]),
grid on,
xlabel('\theta in degrees')
ylabel('Transmit pattern at \phi = 0 deg in dB')

figure(5) % Figure 19
% plot Two-way pattern of 16x8 subarrays spaced 5 wavelength at H-plane
plot(theta(1:720), dbBAF(1:720,1)),axis([-90 90 -80 0]),
grid on,ylabel('Two-way pattern at \phi = 0 deg in dB'),
xlabel('\theta in degrees')

figure(6) % Figure 20
```

```
% plot Two-way pattern of 16x8 subarrays spaced 5 wavelength at E-plane
plot(theta(1:720), dbBAF(1:720,361)),axis([-90 90 -80 0]),
grid on,ylabel('Two-way pattern at \phi = 90 deg in dB'),
xlabel('\theta in degrees')
% End of DSA.m
%%%%%%%%%%%%%%%%%%%%%%%%%%%%%%%%%%%%%%%%%%%%%%%%%%%

%%%%%%%%%%%%%%%%%%%%%%%%%%%%%%%%%%%%%%%%%%%%%%%%%%%
% IrregSubarray.m
% AF of VHF DSA with freq 100 MHz
% Looking for the locations of 38 optimized element in 4 subarrays
% Find element optimized location and first null by myfun10.m
% All position in wavelengths
% Used for Figure 28, 29 pattern plot


clear all;
u0=0.05; % Initial guess of beamwidth
u1=1;
% element locations of first subarray
s0=0; % Lower boundary of elements in 1st subarray
s11=5.58; % Upper boundary of elements
for n=1:10
   s1(n)=0.5073*n;
end
% Initial guess and boundary of 12 element locations
s10=cat(2,s0,s1,s11);
s1l=cat(2,s0,s1-0.5,s11);
s1u=cat(2,s0,s1+0.5,s11);
```

```
% element locations of 2nd subarray
s21=5.109; % First element position
s26=7.607; % Last element position
for n=1:4
   s2(n)=s21+n*0.49;
end
% Initial guess and boundary of 6 element locations
s20=cat(2,s21,s2,s26);
s2l=cat(2,s21,s2-0.45,s26);
s2u=cat(2,s21,s2+0.45,s26);
% element locations of 3rd subarray
s31=10.7439; % First element position
s37=13.576; % Last element position
for n=1:5
   s3(n)=s31+n*0.472;
end
% Initial guess and boundary of 7 element locations
s30=cat(2,s31,s3,s37);
s3l=cat(2,s31,s3-0.45,s37);
s3u=cat(2,s31,s3+0.45,s37);
% element locations of 4th subarray
s41=11.553; % First element position
s413=17.623; % Last element position
for n=1:11
   s4(n)=s41+n*0.50583;
end
% Initial guess and boundary of 13 element locations
s40=cat(2,s41,s4,s413);
```

```
s4l=cat(2,s41,s4-0.5,s413);
s4u=cat(2,s41,s4+0.5,s413);
% Combination of all element positions
llb=cat(2,u0,s1l,s2l,s3l,s4l);   % lower bound of element and the first null position
lub=cat(2,u1,s1u,s2u,s3u,s4u);   % upper bound of element and the first null position
l0=cat(2,u0,s10,s20,s30,s40);    % Intial guess of element and the first null
options=optimset('MinAbsMax',1);
[l,fval, maxfval, exitflag, output]=fminimax(@myfun10,l0,[],[],[],[],llb,lub,[],options)

% Result pattern calculation
% Scan angle input in degrees
thets=0; phis=0;
us=sin(thets*pi/180)*cos(phis*pi/180);
vs=sin(thets*pi/180)*sin(phis*pi/180);
% x,y direction cosine
thet=linspace(-90,89.75,720);
theta=thet.';
phi=linspace(0,179.75,720);
u=sin(theta*pi/180)*cos(phi*pi/180);
v=sin(theta*pi/180)*sin(phi*pi/180);
U=u-us; V=v-vs;
% AF of optimized location
LAFx=zeros(720);
for lx=1:length(ll)
   psilx=2*pi*ll(lx)*U;
   LAFx=LAFx+exp(j*psilx);
end
dbLAF=20*log10(abs(LAFx)/length(ll));
```

```
db2LF=40*log10(abs(LAFx)/length(ll)); % Equivalent 2way pattern
% Pattern plot of optimized position used on Fig. 28
figure(1)
plot(theta, dbLAF(:,4*phis+1)),axis([-90 90 -60 0]),
grid on,
xlabel('\theta in degrees')
ylabel('Relative pattern in dB')

% Equvalent 2-way pattern used on Fig. 29
figure(2)
plot(theta, db2LF(:,4*phis+1)),axis([-90 90 -60 0]),
grid on,
xlabel('\theta in degrees')
ylabel('Relative pattern in dB')
% end of IrregSubarray.m
%%%%%%%%%%%%%%%%%%%%%%%%%%%%%%%%%%%%%%%%%%%%%%%%%%%%%%


%%%%%%%%%%%%%%%%%%%%%%%%%%%%%%%%%%%%%%%%%%%%%%%%%%%%%%
% myfun10.m
% Function for optimization location of subarrays
% Function called by the IrregSubarray.m
% Minimaxing the peak sidelobe level in the visible region[-pi/2,pi/2]

function F=myfun10(l)
% Array factor of same subarray with irregular spacing
% Computation for U axis only
u0=linspace(l(1),0.5*pi,5000);
alpha=2*l;
```

```
F1=zeros(1,length(u0));

for n=2:39

   F1=F1+exp(j*alpha(n)*u0);

end

F=abs(F1);

% end of myfun10.m

%%%%%%%%%%%%%%%%%%%%%%%%%%%%%%%%%%%%%%%%%%%%%%%%%%%
```

LIST OF REFERENCES

1. Http://www.globalsecurity.org, July 2003.
2. Http://www.Janes.com, the general specification of European Multifunction Phased-Array Radar (EMPAR).
3. Nicholas Fourikis, *Advanced Array System, Application and RF Technologies*, Academic Press, London, 2000.
4. Moor S.A.W. and Moor A.R., "Dual Frequency Multi-Function Radar Antenna Research," Proc. of IEE ICAP 97, 1997.
5. Warren L. Stutzman and Gary A. Thiele, *Antenna Theory and Design*, 2nd edition, Wiley, 1998.
6. Balanis, Constantine A., *Antenna Theory: Analysis and Design*, Wiley, New York, 1997.
7. Warren L. Stutzman and Gary A. Thiele, *Antenna Theory and Design*, pp. 39-40 2nd edition, Wiley, 1998.
8. Amit P. Goffer and Moshe Kam, "Design of Phased Arrays in terms of Random Subarrays," *IEEE Trans. on Antenna and Propagation*, vol. 42, No. 6, June 1994.
9. Sergio Sabatini and Marco Tarantino, *Multifunction Array Radar*, pp. 28-29, Artech House, Boston, 1994.
10. Merrill l. Skolnik, *Introduction to Radar Systems*, McGraw-Hill, New York, 2001.
11. Hans Steyskal, Robert A. Ahore and Randy L. Haupt, "Methods for Null Control and Their Effects on the Radiation Pattern," *IEEE Trans. on Antenna and Propagation*, vol. AP-34, N0. 3, p. 404, March 1986.
12. Roy Streit, "Sufficient Conditions for the Existence of Optimum Beam Pattern for Unequally Spaced Linear Arrays," *IEEE Trans. on Antenna and Propagation*, pp. 112-115, January 1975.

13. Jan O. Erstad and Sverre Holm, "An Approach to the Design of Sparse Array System," *IEEE Ultrasonics Symposium*, pp. 1507-1510, 1994.

14. Hu Hang, "Analysis of Pattern Function of the DBF in Non-uniform Subarrays and a Modified Weighting Method," *IEEE Trans. on Antenna and Propagation*, pp. 1083-1087, 2001.

15. T.W. Parks and J.H. McClellan, "Chebyshev Approximation for Nonrecursive Digital Filters with Linear Phase," *IEEE Trans. Circuit Theory*, vol. 19, pp. 189-194, 1972.

16. Jon A. Bartee, "Genetic Algorithm as a Tool For Phased Array Radar Design," Master's Thesis, Naval Postgraduate School, Monterey, California, 2002.

17. Wille Ng, Andrew A. Walston and Norman Bernstein, "The First Demonstration of an Optically Steered Microwave Phased Array Antenna Using True-Time-Delay," *Journal of Lightwave Technology*, vol. 9., September 1991.

18. Yaron Seliktar, "Space-Time Adaptive Monopulse Processing," Doctoral thesis, Georgia Institute of Technology, 1998.

INITIAL DISTRIBUTION LIST

1. Defense Technical Information Center
   Ft. Belvoir, Virginia

2. Dudley Knox Library
   Naval Postgraduate School
   Monterey, California

3. Chairman
   Information Sciences Department
   Naval Postgraduate School
   Monterey, California

4. Professor David C. Jenn
   Department of Electrical and Computer Engineering
   Naval Postgraduate School
   Monterey, California

5. Professor Richard W. Adler
   Department of Electrical and Computer Engineering
   Naval Postgraduate School
   Monterey, California

6. LTCDR Chih-heng Lin
   Taiwan